

# 000 001 002 003 004 005 006 007 008 009 010 011 012 013 014 015 016 017 018 019 020 021 022 023 024 025 026 027 028 029 030 031 032 033 034 035 036 037 038 039 040 041 042 043 044 045 046 047 048 049 050 051 052 053 MARBLE: A HARD BENCHMARK FOR MULTIMODAL SPATIAL REASONING AND PLANNING

Anonymous authors

Paper under double-blind review

## ABSTRACT

The ability to process information from multiple modalities and to reason through it step-by-step remains a critical challenge in advancing artificial intelligence. However, existing reasoning benchmarks focus on text-only reasoning, or employ multimodal questions that can be answered by directly retrieving information from a non-text modality. Thus, complex reasoning remains poorly understood in multimodal domains. Here, we present MARBLE, a challenging multimodal reasoning benchmark that is designed to scrutinize multimodal language models (MLLMs) in their ability to carefully reason step-by-step through complex multimodal problems and environments. MARBLE is composed of three highly challenging tasks, M-PORTAL, M-CUBE and M-MAZE, that require the crafting and understanding of multistep plans under spatial, visual, and physical constraints. We find that current MLLMs perform poorly on MARBLE—all 12 advanced models obtain around 0% accuracy performance on M-CUBE and M-MAZE, while only Grok-4 and GPT-5 slightly outperformed the random baseline on M-PORTAL. These results indicate that complex reasoning is still a challenge for existing MLLMs. Moreover, we show that perception remains a critical bottleneck to multimodal reasoning. By shedding light on the limitations of MLLMs, we hope that MARBLE will spur the development of the next generation of models with the ability to reason and plan across many multimodal reasoning steps.

## 1 INTRODUCTION

Human reasoning is inherently multimodal and sequential—integrating modalities such as language or vision as context to draw conclusions through structured, step-by-step thought. While LLMs have made significant strides in step-by-step reasoning (Wei et al., 2022; Jaech et al., 2024; Guo et al., 2025; OpenAI, 2025), the multimodal reasoning abilities of Multimodal LLMs (MLLMs) are still in their infancy and not yet well understood. Achieving complex, multi-step, multimodally grounded reasoning is critical for building intelligent systems that can generalize across domains and interact adaptively with complex environments.

Recent benchmarks – such as ScienceQA (Lu et al., 2022), MathVista (Lu et al., 2023b), and MMMU (Yue et al., 2024) – have shown that MLLMs can solve tasks involving both visual and linguistic understanding. However, these benchmarks often emphasize relatively shallow forms of reasoning, such as single-step question answering or factual retrieval. They frequently conflate *perception* (e.g., interpreting an image or diagram) with *reasoning* (e.g., drawing logical inferences, comparing evidence, or crafting a multi-step plan), reducing complex reasoning to pattern matching and multimodal integration. As a result, current evaluations underexplore and undermeasure an MLLM’s capacity for deep, structured reasoning. Moreover, the recent literature has focused heavily on abstract reasoning in domains such as advanced mathematics or code generation, where multimodal embodiment plays a limited role. In contrast, interacting with and planning in spatially and physically constrained environments is a fundamental dimension of human intelligence but it is largely missing from today’s MLLM evaluations. While a recent effort introduced an escape room-inspired benchmark (Wang et al., 2025b), frontier models were not sufficiently challenged by its task complexity, achieving up to 100% escape rate. Thus, hard benchmarks that stress multi-step planning and spatial reasoning under physical constraints remain an open need. Analogous to how difficult challenges have historically driven progress, we believe that an ARC-like test (Chollet et al., 2024) for multimodal reasoning could spark foundational advances in MLLM capabilities.

054  
055 Table 1: Conceptual overview of the MARBLE benchmark.  
056  
057  
058  
059  
060  
061  
062  
063  
064  
065  
066

Dataset	Description	Subtasks	# Samples	Metrics
M-PORTAL	Solving complex multi-modal spatial reasoning and planning problems.	Plan correctness, Fill-the-blanks	512 512	F1-Score, Accuracy
M-CUBE	Assembling 3D Cube from six jigsaw pieces.	CUBE, CUBE-easy	1,000 1,000	Accuracy
M-MAZE	Solving dynamic mazes by combining tile insertion and player navigation.	MAZE, MAZE-easy	1,000 1,000	Success Rate

067 In this work, we present MARBLE (MultimodAI Reasoning Benchmark for Language modEls), a  
068 highly challenging multimodal reasoning benchmark specifically designed to evaluate step-by-step,  
069 multimodally grounded reasoning in MLLMs. Our benchmark introduces tasks that are cognitively  
070 demanding, requiring models to decompose complex multimodal prompts into interpretable intermediate  
071 steps, align information across inputs, and to carefully craft a multi-step plan to solve complex  
072 problems under diverse spatial and physical constraints. Unlike prior datasets that overemphasize  
073 final-answer accuracy, our benchmark emphasizes reasoning trajectories and plans, providing both  
074 gold-standard rationales and mechanisms for evaluating intermediate step fidelity. MARBLE  
075 consists of three main tasks, M-PORTAL which tests complex spatial reasoning and planning abilities,  
076 M-CUBE, which tests the ability to understand and assemble 3D jigsaw pieces into a target cube  
077 shape, and M-MAZE, which test the ability to plan the path to target in an editable maze. Each  
078 dataset also contains two subtasks at different difficulty levels, as shown in Table 1.

079 We conduct an extensive evaluation of MARBLE across 12 state-of-the-art MLLMs and reasoning  
080 models. Intriguingly, most models obtain near-random performance on M-PORTAL and around  
081 0% accuracy on M-CUBE and M-MAZE. Even in simplified configurations, only about half of  
082 the models are able to outperform the random baseline. Notably, Grok-4 and GPT-5 are the only  
083 model demonstrating reasonable performance on M-PORTAL, achieving 18.2% and 14.2% F1 score,  
084 respectively. However, they still completely fail on the harder tasks of M-CUBE and M-MAZE.  
085 These results indicate that complex multimodal reasoning remains a significant challenge for current  
086 MLLMs. Our further analysis shows that perception is still a bottleneck for multimodal reasoning:  
087 all the advanced MLLMs completely fail to understand and extract structured information from the  
088 visual inputs. Additionally, we present an interactive setup for M-CUBE and M-MAZE to help the  
089 multimodal reasoning via the feedbacks from the environments, reflecting the real-world and agentic  
090 problem-solving processes. We hope that MARBLE will serve as a probing benchmark to reveal the  
091 limitations of current MLLMs and drive the development of next-generation models with stronger  
092 capabilities in multi-step multimodal reasoning and planning.

## 093 094 2 MARBLE: A BENCHMARK FOR MULTIMODAL SPATIAL REASONING AND 095 PLANNING

096  
097  
098 We present MARBLE, a challenging game-inspired multimodal reasoning benchmark designed to  
099 evaluate the complex reasoning abilities of multimodal LLMs (MLLMs). In contrast to prior reasoning  
100 benchmarks that evaluate only the final answer independent of the reasoning trace, MARBLE focuses  
101 on assessing the correctness of the reasoning process itself. MARBLE consists of three tasks, M-  
102 PORTAL, M-CUBE and M-MAZE, all require complex, multi-step and multimodal reasoning skills  
103 to forge an appropriate plan that accounts for complex spatial and physical problem constraints.  
104 The M-PORTAL task challenges MLLMs to solve problems derived from Portal 2 videogame with  
105 multi-step reasoning and planning. The M-CUBE evaluates MLLMs in their ability to solve Happy  
106 Cube puzzles, *i.e.*, rotate complex shapes to arrange them into 3D cubes under physical constraints.  
107 Finally, the M-MAZE tests the ability of MLLM to plan the correct path to the target, in a dynamic  
108 and editable maze.

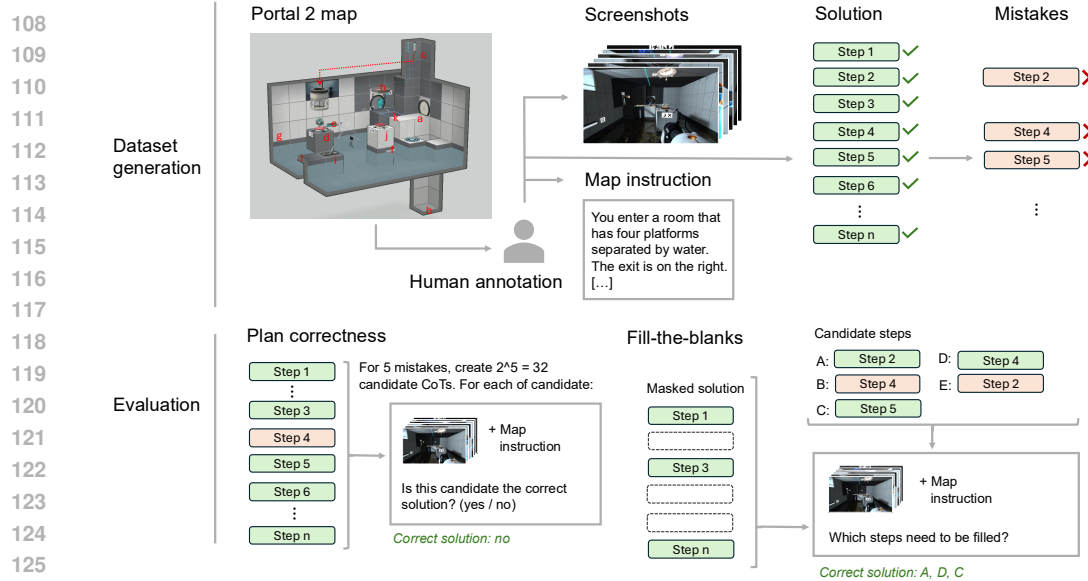


Figure 1: Data generation and evaluation pipeline for the M-PORTAL task. The top row illustrates how a given Portal 2 map (sourced from the community test chambers) was analyzed with human annotation to produce a set of illustrative screenshots that fully depict the map, textual map instructions, a ground-truth solution chain of thought (CoT), as well as a set of five mistaken steps. The steps are designed to operate independently so that mistakes and correct steps can be easily combined. The bottom row indicates two evaluation types of M-PORTAL: first, plan correctness, a binary evaluation where candidate solutions have to be rated as correct or wrong. Second, a fill-the-blanks evaluation, where multiple steps of the ground truth CoT solution are masked, and multiple options are available to fill in at the right place.

## 2.1 M-PORTAL

The M-PORTAL task is a multimodal reasoning task that involves planning, spatial reasoning, as well as multimodal integration. M-PORTAL is inspired by the game Portal 2, a first-person perspective puzzle videogame released by Valve in 2011. Portal challenges players to overcome obstacles and to pass through rooms by means of placing two portals through which players can teleport. A key mechanic in Portal is the conservation of momentum: when a player enters one portal with a given velocity, they exit the second portal with the same relative momentum. This enables creative traversal strategies, such as jumping across large gaps or over obstacles, by combining gravity-driven falls with portal placement. Various additional features (*e.g.*, buttons, lasers, tractor beams, liquids) add further complexity to the puzzle environments. The ultimate trial will be for MLLMs to interactively navigate and solve the game. However, to enable broad accessibility and usability of this benchmark, we abstract a given map into a set of visual question-answering tasks that require the MLLM to integrate several depictions of the map, a textual instruction to the map, in order to examine partial or complete chain of thought (CoT) solution plans that may consist of dozens of steps. Figure 8 in Appendix D gives an introductory overview of how a basic portal map could look like, displaying a scene overview (top left), the step-by-step solution, and a few in-game screenshots.

**Problem statement.** Given an input  $X = (\mathcal{I}, T)$ , where  $\mathcal{I}$  is a set of multimodal inputs (*e.g.*, screenshots of a Portal map or textual contextualization of the environment) and  $T$  is a task instruction, the objective is to generate a Chain-of-Thought (CoT) plan  $P = (s_1, s_2, \dots, s_n)$  consisting of interpretable, physically sound reasoning steps that, if executed, would successfully solve the problem. The reward of a plan  $R(P)$  is 1 if the exit door is passed, and 0 otherwise. Then the objective is to evaluate the ability of models to implement the mapping  $F^*$  that maximizes the reward, *i.e.*,

$$F^* = \arg \max_F \mathbb{E}_{X \sim \mathcal{D}} [R(F(X))], \text{ where} \quad (1)$$

$$F : X \mapsto P = (s_1, s_2, \dots, s_n). \quad (2)$$

162 **Data collection.** For data collection, a human annotator with advanced Portal 2 experience browsed  
 163 through top-rated maps from the Portal 2 community test chambers. We focused on the community  
 164 test chambers, as they were often self-contained, well-defined problems in a single room. The  
 165 annotator selected 16 high-quality maps that received top user-rating, while being compactly shaped  
 166 such that they would be amenable to capture within a few screenshots. Figure 1 gives an overview  
 167 of how the  $\mathbb{M}$ -PORTAL dataset was created in the top row, whereas the bottom row indicates the  
 168 evaluation strategies employed in the  $\mathbb{M}$ -PORTAL task.

169 **Evaluation subtasks.** Since direct execution and success validation in the Portal environment  
 170 would depend on a closed-source game environment and could involve a brittle interfacing and  
 171 limited accessibility, we focus on evaluating the ability of a model to reason about the correctness of  
 172 candidate plans or the missing steps in incomplete plans. For this, we consider two types of closed-  
 173 ended evaluations: `plan correctness` and `fill-the-blanks` tasks, each contributing to  
 174 512 problems.

175 **1. Plan correctness:** *Is the provided candidate plan correct?*

176 Plan correctness is the binary classification task and requires answering yes/no questions. It  
 177 is a harder task compared to fill-the-blanks because models have to carefully review lengthy  
 178 candidate plans that may be dozens of steps long and involve various spatial and physical  
 179 constraints and dependencies. These candidates may contain no mistake at all up until five  
 180 mistaken steps. This task has a significant class imbalance, as one Portal map with five  
 181 available mistaken steps allows the creation of  $2^5 = 32$  candidates that leverage individual  
 182 mistakes, whereas only one out of 32 candidates is correct.

183 **2. Fill-the-blanks:** *Can the model accurately identify several missing steps given surrounding  
 184 context and a few candidate options?*

185 On the easier fill-the-blanks task, models receive a partial plan to solve the Portal map  
 186 whereas several steps are masked. To fill the missing steps, the model needs to choose five  
 187 correct options from five mistake or distracting options in a correct order. Even though this  
 188 task is hard for a naive random baseline, for a model that is able to interpret the multimodal  
 189 inputs  $X$  as well as the partial solution, it should be easier to identify the correct missing  
 190 steps especially since mistaken steps also appear in their correct version as highly similar  
 191 options. Furthermore, fill-the-blanks can also be seen as a simplification as it helps the  
 192 model focus its attention on a few relevant steps out of a large sequence, whereas in the  
 193 binary evaluation any step could be potentially mistaken.

194 **2.2  M-CUBE**

195 **Problem statement.** The  $\mathbb{M}$ -CUBE task is a 3D spatial puzzle inspired by the Happy Cube, a  
 196 mechanical puzzle originally invented by Dirk Laureysens in 1986. In this task, one is presented with  
 197 6 jigsaw-style pieces taken from the faces of a  $5 \times 5 \times 5$  Cube. Each piece is featured by the bump  
 198 and gap pattern on its edges. The goal is to assemble the pieces into a valid cube where the edges are  
 199 aligned seamlessly without gap or overlap. To solve the  $\mathbb{M}$ -CUBE task, an MLLM needs to assign  
 200 each piece into a cube face with proper orientation, *i.e.*, to rotate and/or flip the piece accordingly  
 201 to align with other pieces. For each problem, an MLLM must account for  $6!$  possible piece-to-face  
 202 assignments (modulo rotational symmetries), and for each piece, 8 discrete states of rotations and  
 203 flips, resulting in a combinatorial explosion of candidate solutions. Among the vast search space,  
 204 only very few solutions are valid given the geometric constraints imposed by the interlocking bump  
 205 and gap patterns. András et al. (2013) reported that most commercially available cubes have only one  
 206 solution (up to rotational equivalences), making this a challenging reasoning problem.

207 **Data generation.** While the  $\mathbb{M}$ -CUBE tasks are inspired by the Happy Cube puzzle, we generate all  
 208 samples synthetically. Figure 2 gives an overview of the workflow. Specifically, the data generation  
 209 pipeline starts with a  $5 \times 5 \times 5$  cube and disassembles the surface into 6 interlocking pieces. Each  
 210 piece can be regarded as a  $5 \times 5$  grid, where the center  $3 \times 3$  region is always preserved. For  
 211 remaining cells located on the edges, we randomly assign each cell to one of the adjacent faces of  
 212 the big  $5 \times 5 \times 5$  cube, to create the bump and gap patterns along the boundary. After that, the  
 213 obtained pieces are shuffled and rendered from a random 3D viewpoint as the input to an MLLM. We  
 214 interactively selected viewpoint ranges such that the shape was clearly discernible. Concretely, we

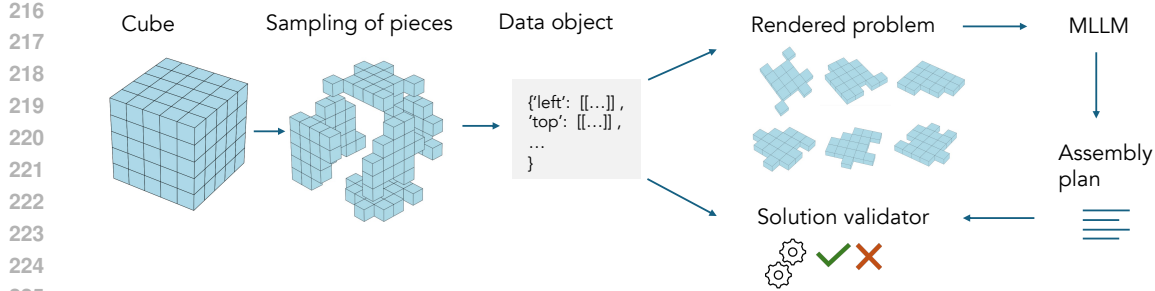


Figure 2: Overview of the M-CUBE workflow including data generation, problem rendering, as well as solution validation.

render the objects by sampling a camera elevation in the range of  $-155^\circ$  to  $-115^\circ$  and an azimuth in the range of  $-150^\circ$  to  $-90^\circ$ , relative to the canonical front view. The base view corresponds to an elevation of  $-135^\circ$  and an azimuth of  $-120^\circ$ , with uniformly random perturbations of  $\pm 20^\circ$  and  $\pm 30^\circ$ , respectively.

**Solution validator.** The model is required to find the correct piece-to-face mapping and the orientation of 6 pieces. However, for each problem, there is no unique solution since a cube contains 24 rotational symmetries. Therefore, instead of directly comparing the answer to ground-truth, we provide a solution validator by testing whether the solution from MLLM could successfully assemble the pieces into a perfect cube. Beside binary evaluation, the solution validator could also identify the conflicts in a given configuration, such as mismatched edges. This diagnostic feedback can be used by an MLLM to iteratively refine its solution. See Appendix D.2 for example.

**Evaluation subtasks.** To measure the performance of MLLMs with controlled difficulty level, we create two subtasks called CUBE and CUBE-easy. Each subtask contains 1000 examples. CUBE-easy is a simplified version of CUBE along three axes: *i*) the input pieces are represented as 2D arrays instead of the rendered image to reduce the perception error of MLLM (see the discussion in Section 3.2 for more details); *ii*) each puzzle is specially designed such that the solution does not require flipping of any pieces; *iii*) a partial solution with the arrangement of 4 pieces is provided in the prompt, leaving only 2 missing pieces to be placed. Consequently, *ii*) and *iii*) significantly reduce the size of search space. In comparison, CUBE retains the full complexity of the task, where the MLLM needs to understand the input images, and explore over all the possible arrangements of the 6 pieces.

### 2.3 M-MAZE

**Problem statement.** The M-MAZE task is 2D spatial-planning puzzle directly inspired by *The aMAZEing Labyrinth* board game. Each game contains a  $7 \times 7$  maze and one off-board *spare* tile. The tile contains three shapes I/L/T and can have different orientations on the board. There are two types of actions in the action space: (i) *insert* the spare tile into one row or column to shift the whole line (ii) *move* along connected corridors. The *insert* action will change the connectivity of the board and make the maze dynamic. Given a board image, a model must produce a valid multi-turn plan to move the player to the target, which poses unique challenges to MLLMs in terms of perception and multi-step reasoning.

**Data generation.** Similar to M-CUBE, we synthesize M-MAZE tasks by generating initial board configurations, starting with 16 fixed path tiles and 12 fixed treasures, then sampling the remaining I/L/T tile shapes, random player positions, and 12 scattered treasures to complete the board. The process begins with board sampling, followed by BFS to compute all trajectories to each target via TILE INSERTION (shifting rows/columns) and PLAYER MOVE (along connected tiles), determining minimal depth  $D$  (the fewest turns to reach a target). We subsample trajectories by  $D$ , a difficulty proxy since higher  $D$  increases the search space and planning complexity, and retain one solution per  $(board, seed, depth)$  triplet for diversity. Evaluation uses only the initial configuration (board grid, player position, and target, excluding other objects to reduce clutter), providing a lower bound on the planning depth required to solve the puzzle.

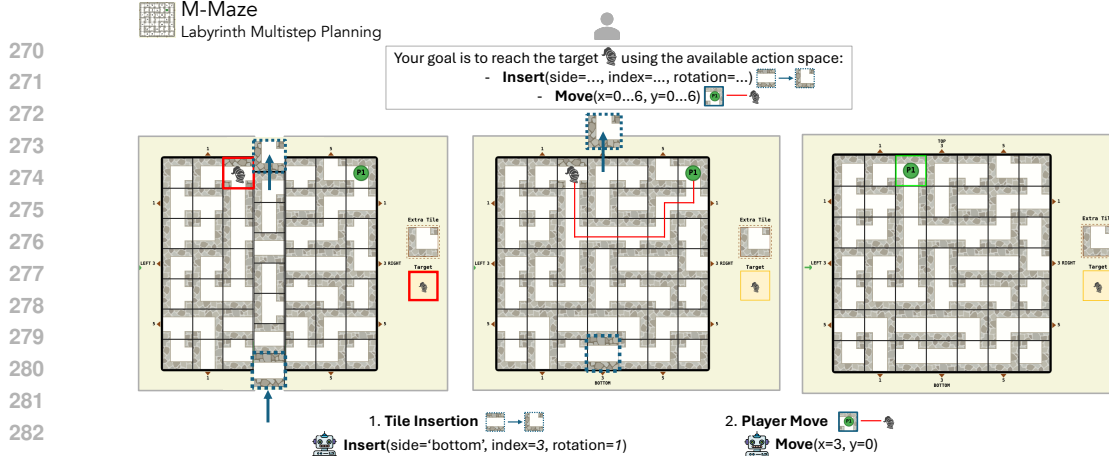


Figure 3: Overview of the M-MAZE task.

**Evaluation subtasks.** Similar to M-CUBE, we create two subtasks to measure the performance of MLLM with controlled difficulty levels: MAZE and MAZE-easy. Each subtask contains 1000 examples. MAZE-easy is a simplified version of MAZE along two axes: *i*) the input board includes a **visual harness** overlay (tile types and coordinates) and the full symbolic state (board grid, object grid, extra tile, player position); *ii*) a reduced depth  $D = 2$ . These adjustments minimize perception errors and shrink the search space. In contrast, MAZE retains full complexity at depth  $D = 4$ , requiring the MLLM to interpret the raw board image demanding deep planning and strong visual parsing capabilities.

### 3 EXPERIMENTS

We evaluate performance on the MARBLE benchmark using eight state-of-the-art MLLMs, including both open-source and closed-source models with advanced multimodal reasoning capabilities. Specifically, we assess three representative open-source MLLMs: Qwen2.5-VL-72B (Bai et al., 2025), InternVL3-78B (Zhu et al., 2025) and Llama-4-Scout (Meta, 2025), alongside eight closed-weight models: GPT-4o (Hurst et al., 2024), GPT-o3, GPT-o4-mini, GPT-5, Claude-3.7-Sonnet (Anthropic, 2025) Gemini-2.5-pro (Google DeepMind, 2025), Seed1.5-VL Team (2025) and Grok-4. In addition, we also include one text-only model DeepSeek-R1-0528 Guo et al. (2025) in the evaluation. We remove or manually convert the input images into textual descriptions to evaluate the models that only takes text inputs. Besides, we provide evaluation of experienced human players on all the tasks. All the experiment configurations, prompts and hyperparameters are detailed in the Appendix E. Experiments are conducted on a single node server with 8 Nvidia H200 GPUs. The overall results are reported at Table 6.

#### 3.1 RESULTS ON M-PORTAL

We evaluate state-of-the-art MLLMs on the `plan correctness` and `fill-the-blanks` tasks of the M-PORTAL, as reported in Table 6. On the `plan correctness` task, all the investigated models (except GPT-5 and Grok-4) performed very poorly with a minority class F1 score of around 6%, similar to the random baseline. In comparison, on the easier `fill-the-blanks` task, 8 out of 12 models outperform the random baseline. In particular, the performance gap compared to the random baseline is substantial ( $\geq 20\%$ ) for Gemini-2.5-pro, GPT-o3, Grok-4 and GPT-5 that significantly outperforms all other models. Interestingly, the best performing model, Grok-4, manages to correctly solve only 46.7% of the problems on `fill-the-blanks` tasks and achieves 18.2% F1 score on the `plan - correctness` binary classification. Note that although the `fill-the-blanks` task results in random baseline scores, it is expected to be easier than the `plan correctness` task for models capable of interpreting the multimodal inputs and leveraging the partial solution. Also, it's worth noting that the experienced human player could obtain 37.5% on the `fill-the-blanks` subtask, surpassing all the frontier models except Grok-4.

Table 2: Performance of state-of-the-art MLLMs on the MARBLE benchmark and three tasks: M-PORTAL, M-CUBE and M-MAZE. Each task contains two difficulty levels. We report F1-score (%) for binary evaluation (plan correctness) of M-PORTAL and success rate (%) for all the other tasks. Human performance was evaluated with 2–3 experienced players on each task. \*All the visual inputs are removed or converted to texts for text-only LLMs.

Models	M-PORTAL		M-CUBE		M-MAZE	
	Binary	Blanks	CUBE	CUBE-easy	MAZE	MAZE-easy
Human	-	37.5	0.0	85.0	55.0	80.0
Random	6.1	3e-3	1e-5	3.1	5e-9	1e-4
<i>Open-weights models</i>						
Qwen2.5-VL-72B	6.6	0.0	0.0	2.0	0.0	0.1
InternVL3-78B	6.4	0.0	0.0	2.8	0.0	0.0
Llama-4-Scout	6.5	0.0	0.0	1.6	0.0	0.3
Seed1.5-VL	7.6	4.1	0.0	2.0	0.0	0.0
DeepSeek-R1-0528*	0.0	10.0	0.0	8.0	0.0	2.0
<i>Closed-weights models</i>						
Claude-3.7-Sonnet	6.3	8.8	0.0	7.4	0.0	1.0
Gemini-2.5-Pro	4.7	20.0	0.0	11.0	0.0	20.0
GPT-4o	6.5	0.4	0.0	2.0	0.0	0.0
o4-mini	0.0	5.5	0.0	16.0	<b>1.0</b>	23.0
o3	6.6	23.4	0.0	72.0	0.0	69.0
GPT-5	14.2	29.1	0.0	<b>84.0</b>	0.0	66.0
Grok-4	<b>18.2</b>	<b>46.7</b>	0.0	38.6	0.0	47.0
Grok-4 Fast	15.1	31.0	0.0	53.0	0.0	<b>75.0</b>

**Influence of blanks.** In the fill-the-blanks task on M-PORTAL, each question contains multiple steps in the complete solution, and part of them are masked. To systematically understand the impact of missing information, we construct a series of questions where the model is asked to fill  $n$  blanks from  $2n$  candidate options. We evaluate the performance of Qwen2.5-VL-72B and the result is shown in Figure 4. Notably, the model obtains around 70% accuracy when only a single blank is present. However, the performance declines rapidly as the number of blanks increases, dropping to less than 1% when  $n \geq 4$ , which indicates the challenges of the subtask under the conditions of extensive missing information.

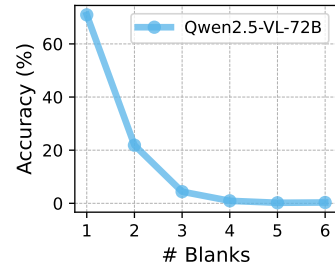


Figure 4: The influence of number of blanks to M-PORTAL.

### 3.2 RESULTS ON M-CUBE

The results on the CUBE and CUBE-easy tasks of M-CUBE are shown in Table 6. Intriguingly, all the advanced MLLMs completely fail on the harder subtask CUBE and obtain 0% accuracy despite more than 10,000 tokens spent on thinking the problems. The results highlight the complex multimodal reasoning process involved in CUBE, where the model has to iterate over verification and backtracking through a long reasoning chain to make a final answer. In comparison, on the simplified CUBE-easy task, 7 out 12 frontier models are able to perform better than random guess. Among them, GPT-5 and GPT-03 achieves remarkable performance of 84.0% and 72.0 accuracies, substantially outperforming the remaining models, but are still slightly worse than the human performance of 85.0% accuracy.

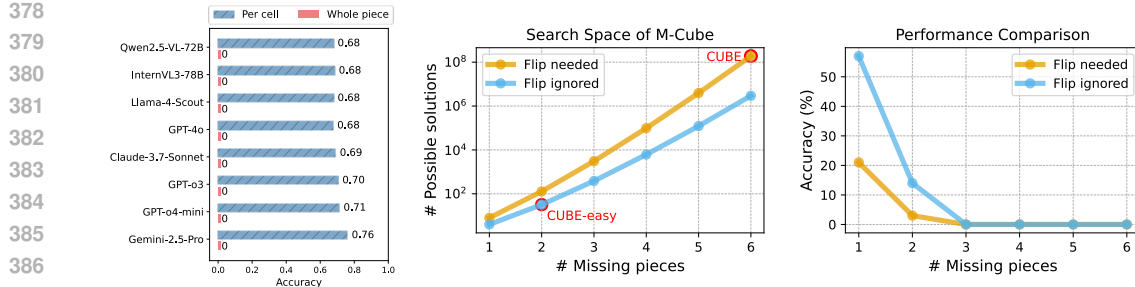


Figure 5: *Left*: Perception remains a bottleneck for M-CUBE. A perception task designed to test MLLM’s ability on retrieve structured information from visual input (full prompt in Appendix D.2). : *Middle*: Search space of the M-CUBE dataset under different configurations. *Right*: Performance of DeepSeek-R1 across varying levels of task difficulty of the M-CUBE dataset.

**Error on perception.** To solve the M-CUBE puzzle, the first step is to understand the visual input and retrieve the relevant information, which serves as the basis of the reasoning steps afterwards. Thus, we design a perception task to measure whether the MLLMs could correctly extract information from the input image: given a jigsaw-style piece in a 3D viewpoint, the model is asked to convert the piece into a  $5 \times 5$  array. We evaluate all the 8 MLLMs on this perception task with 200 test examples, and report the accuracy on cells and accuracy of the whole piece also on Figure 5 left. Surprisingly, we found all the models could only achieve around 70% accuracy per cell. The best perception performance, is 76% accuracy from Gemini-2.5-pro, meaning that the model could still occasionally make mistakes. As a result, all the models achieve 0% accuracy on the whole piece. These results highlight that even advanced MLLMs struggle with this seemingly simple perception task, posing a potential bottleneck for multimodal reasoning in complex scenarios like CUBE.

**Error on reasoning.** Apart from the perception errors, M-CUBE still remains a highly challenging problem due to the vast search space from the combination of all possible arrangements and orientations of 6 pieces. Figure 5 illustrates the size of search space of M-CUBE as a function of both the number of missing pieces and whether a solution requires flipping the pieces. In particular, CUBE comprises  $6! * 8^6 = 188,743,680$  possible solutions. In comparison, CUBE-easy only contains 32 possible solutions, a 5,000,000 fold reduction of the hypothesis space. To isolate the reasoning challenge from perceptual limitation, we manually convert the visual inputs into corresponding text arrays. We then compare the performance of DeepSeek-R1 in different search space configurations, as shown in Figure 5. The model obtains 57% accuracy in the simplest setting with only one missing piece. However, the performance drops drastically as the search space expands, falling to 0% when more than 3 pieces are missing. The substantial decline underscores the difficulty of reasoning among expanding combinatorial search space, a major bottleneck for existing reasoning models. In summary, besides perception error, reasoning among the vast search space is also a challenge, making M-CUBE an especially difficult task for state-of-the-art MLLMs.

### 3.3 RESULTS ON M-MAZE

We evaluate state-of-the-art MLLMs on M-MAZE (MAZE, MAZE-easy) as reported in Table 6. Similarly, all the models performs around 0% on the harder subtask, while on the simper subtask MAZE-easy, GPT-o3, Grok-4, GPT-5 are the models significantly outperforming the other models. Interestingly, there is a clearly performance gap between human player and MLLMs on this task: human achieves remarkably 55.0% on MAZE, 80.0% on MAZE-easy, respectively. Moreover, we observe similar perception bottleneck as M-CUBE where MLLM struggles on extracting the structured visual information from the input. We defer the empirical results to the Appendix F.5.2.

**Error on Reasoning.** Beyond perception errors, M-MAZE challenges models due to the need to reason over state transitions and rules across multiple steps, not just static layouts. To isolate reasoning from perception, we use a *Visual Harness + Symbolic* setup, providing the board state in two forms: a compact symbolic grid as text in the prompt, and the input image with labels overlaid directly onto the board (see Figure 15 in Appendix D). We evaluate GPT-5-MINI, with results in Figure 6: 100% success at  $D = 0$ , 70% at  $D = 1$ , 30% at  $D = 2$ , 15% at  $D = 3$ , and below

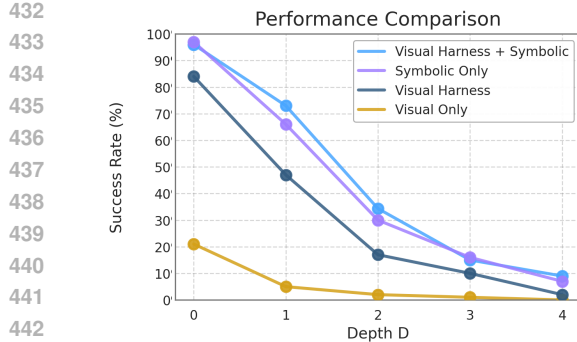


Figure 6: Success rate (%) of GPT-5-mini across depths  $D$  on M-MAZE, comparing four input settings described in Figure 15 in Appendix D.

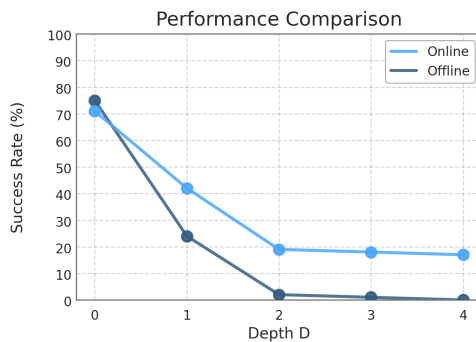


Figure 7: Success rate (%) of GPT-5-nano on M-MAZE using Visual Harness + Symbolic, across depths, comparing Online vs. Offline settings.

10% at  $D = 4$ . The steep decline with depth, driven by error accumulation, highlights several of the most frequent failure modes: (i) **adjacency misinterpretation errors**, where a model either misjudges non-reciprocal openings as being connected or hallucinates a change in a tile’s type to force a valid path, leading to illegal player movement; (ii) **state-update errors**, where the model incorrectly processes a row/column shift by failing to also update the positions of players or items on the affected tiles, leading to an incorrect internal representation of the board state; (iii) **insert legality errors**, a form of instruction-following error, where models attempt illegal moves like using the wrong slots; and (iv) **shallow planning errors**, where a model fails to find a solution and does not output any plan. The steep drop with depth indicates that multi-step reasoning over dynamic, rule-bound states is inherently hard. In summary, beyond perception, planning across multiple turns in a large combinatorial space makes M-MAZE a challenging task for current MLLMs.

**Online Evaluation** We evaluate GPT-5-NANO in a per-action loop: at each phase the agent emits one atomic action (INSERT or MOVE); the environment executes it and returns the next observation. Episodes end on success, illegality (no-reverse, lane legality, invalid move), or budget exhaustion. We report **Success Rate@ $B$**  with  $B = 2D$ , where  $D$  is the optimal depth (two actions per optimal turn: INSERT+MOVE). Results (Fig. 7) show around 80% at  $D=0$  and **online surpassing offline once multi-step planning is required**: around 42% vs. 24% at  $D=1$ , around 19% vs. 2% at  $D=2$ ; online then plateaus at around 17–18% for  $D=3$ –4 while offline collapses to 0%. Overall, step-wise state updates mitigate error accumulation, but performance still degrades with increasing depth, indicating persistent bottlenecks in multi-step transition modeling, spatial consistency, and rule adherence.

## 4 DISCUSSION

This paper introduces MARBLE, a hard multimodal reasoning benchmark for MLLMs. MARBLE provides a focused testbed for evaluating MLLMs on complex spatial reasoning and planning tasks that are underlying heterogenous physical constraints. Our tasks are designed such that an MLLM must first understand the physical constraints imposed by the multimodal input, and then formulate a coherent, multi-step plan that draws from a vast search space in order to solve the problem. MARBLE fills the gap of multimodal reasoning evaluation by shifting the focus from outcome accuracy to process-oriented, multi-steps reasoning that requires coherent multimodal understanding. By contributing a challenging benchmark for multi-step, multimodal reasoning amidst spatial and physical constraints, MARBLE aspires to elicit more progress and innovation in MLLM development that will unlock unprecedented abilities in reasoning and planning amidst complex and multimodal environments—capabilities that are essential for real-world, embodied, and general-purpose intelligence.

Our empirical evaluation reveals that state-of-the-art MLLMs struggle significantly with MARBLE. Most of the models can only outperform random baselines in simplified ablations and fail even on structured perception tasks, underscoring limitations in both reasoning and visual understanding.

486     **Limitations and future work.** We do not explore fine-tuning or adapting models at test time.  
 487     Future work should investigate adaptive approaches, enabling models to reason *with* and *through*  
 488     different modalities—such as “thinking with images”—in a more compositional way.  
 489

490     REFERENCES  
 491

492     Szilárd András, Kinga Sipos, and Anna Soós. *Which is harder?-Classification of Happy Cube puzzles*.  
 493     2013.

494     Anthropic. Anthropic 3.7 Sonnet and Claude Code, February 2025. URL <https://www.anthropic.com/news/clause-3-7-sonnet>.

495     Shuai Bai, Keqin Chen, Xuejing Liu, Jialin Wang, Wenbin Ge, Sibo Song, Kai Dang, Peng Wang,  
 496     Shijie Wang, Jun Tang, et al. Qwen2.5-VL technical report. *arXiv preprint arXiv:2502.13923*,  
 497     2025.

498     Jiacheng Chen, Tianhao Liang, Sherman Siu, Zhengqing Wang, Kai Wang, Yubo Wang, Yuansheng  
 499     Ni, Wang Zhu, Ziyan Jiang, Bohan Lyu, et al. MEGA-Bench: Scaling multimodal evaluation to  
 500     over 500 real-world tasks. *arXiv preprint arXiv:2410.10563*, 2024.

501     Yew Ken Chia, Vernon Toh Yan Han, Deepanway Ghosal, Lidong Bing, and Soujanya Poria. Puz-  
 502     503     zleVQA: Diagnosing multimodal reasoning challenges of language models with abstract visual  
 504     505     patterns. *arXiv preprint arXiv:2403.13315*, 2024.

506     Francois Chollet, Mike Knoop, Gregory Kamradt, and Bryan Landers. Arc prize 2024: Technical  
 507     508     report. *arXiv preprint arXiv:2412.04604*, 2024.

509     Google DeepMind. Gemini 2.5: Our most intelligent ai model, March  
 510     511     2025. URL <https://blog.google/technology/google-deepmind/gemini-model-thinking-updates-march-2025/#gemini-2-5-thinking>.

512     Daya Guo, Dejian Yang, Haowei Zhang, Junxiao Song, Ruoyu Zhang, Runxin Xu, Qihao Zhu,  
 513     514     Shirong Ma, Peiyi Wang, Xiao Bi, et al. Deepseek-R1: Incentivizing reasoning capability in llms  
 515     via reinforcement learning. *arXiv preprint arXiv:2501.12948*, 2025.

516     Yunzhuo Hao, Jiawei Gu, Huichen Will Wang, Linjie Li, Zhengyuan Yang, Lijuan Wang, and  
 517     518     Yu Cheng. Can MLLMs reason in multimodality? EMMA: an enhanced multimodal reasoning  
 519     benchmark. *arXiv preprint arXiv:2501.05444*, 2025.

520     Aaron Hurst, Adam Lerer, Adam P Goucher, Adam Perelman, Aditya Ramesh, Aidan Clark, AJ Os-  
 521     522     trow, Akila Welihinda, Alan Hayes, Alec Radford, et al. Gpt-4o system card. *arXiv preprint  
 523     arXiv:2410.21276*, 2024.

524     Aaron Jaech, Adam Kalai, Adam Lerer, Adam Richardson, Ahmed El-Kishky, Aiden Low, Alec  
 525     526     Helyar, Aleksander Madry, Alex Beutel, Alex Carney, Alex Iftimie, Alex Karpenko, Alex Tachard  
 527     Passos, Alexander Neitz, Alexander Prokofiev, Alexander Wei, Allison Tam, Ally Bennett,  
 528     Ananya Kumar, Andre Saraiva, Andrea Vallone, Andrew Duberstein, Andrew Kondrich, Andrei  
 529     Mishchenko, Andy Applebaum, Angela Jiang, Ashvin Nair, Barret Zoph, Behrooz Ghor-  
 530     bani, Ben Rossen, Benjamin Sokolowsky, Boaz Barak, Bob McGrew, Borys Minaiev, Botao  
 531     Hao, Bowen Baker, Brandon Houghton, Brandon McKinzie, Brydon Eastman, Camillo Lu-  
 532     533     garesi, Cary Bassin, Cary Hudson, Chak Ming Li, Charles de Bourcy, Chelsea Voss, Chen Shen,  
 534     Chong Zhang, Chris Koch, Chris Orsinger, Christopher Hesse, Claudia Fischer, Clive Chan, Dan  
 535     Roberts, Daniel Kappler, Daniel Levy, Daniel Selsam, David Dohan, David Farhi, David Mely,  
 536     David Robinson, Dimitris Tsipras, Doug Li, Dragos Oprica, Eben Freeman, Eddie Zhang, Ed-  
 537     mund Wong, Elizabeth Proehl, Enoch Cheung, Eric Mitchell, Eric Wallace, Erik Ritter, Evan  
 538     Mays, Fan Wang, Felipe Petroski Such, Filippo Raso, Florencia Leoni, Foivos Tsimpourlas, Fran-  
 539     540     cis Song, Fred von Lohmann, Freddie Sulit, Geoff Salmon, Giambattista Parascandolo, Gildas  
 541     Chabot, Grace Zhao, Greg Brockman, Guillaume Leclerc, Hadi Salman, Haiming Bao, Hao  
 542     Sheng, Hart Andrin, Hessam Bagherinezhad, Hongyu Ren, Hunter Lightman, Hyung Won Chung,  
 543     Ian Kivlichan, Ian O’Connell, Ian Osband, Ignasi Clavera Gilaberte, and Ilge Akkaya. Ope-  
 544     nai o1 system card. *CoRR*, abs/2412.16720, 2024. doi: 10.48550/ARXIV.2412.16720. URL  
 545     <https://doi.org/10.48550/arXiv.2412.16720>.

540 Woosuk Kwon, Zhuohan Li, Siyuan Zhuang, Ying Sheng, Lianmin Zheng, Cody Hao Yu, Joseph E.  
 541 Gonzalez, Hao Zhang, and Ion Stoica. Efficient memory management for large language model  
 542 serving with pagedattention. In *Proceedings of the ACM SIGOPS 29th Symposium on Operating  
 543 Systems Principles*, 2023.

544 Bo Li, Yuanhan Zhang, Dong Guo, Renrui Zhang, Feng Li, Hao Zhang, Kaichen Zhang, Peiyuan  
 545 Zhang, Yanwei Li, Ziwei Liu, et al. Llava-onevision: Easy visual task transfer. *arXiv preprint  
 546 arXiv:2408.03326*, 2024.

548 Pan Lu, Swaroop Mishra, Tanglin Xia, Liang Qiu, Kai-Wei Chang, Song-Chun Zhu, Oyvind Tafjord,  
 549 Peter Clark, and Ashwin Kalyan. Learn to explain: Multimodal reasoning via thought chains for  
 550 science question answering. *Advances in Neural Information Processing Systems*, 2022.

551 Pan Lu, Hritik Bansal, Tony Xia, Jiacheng Liu, Chunyuan Li, Hannaneh Hajishirzi, Hao Cheng,  
 552 Kai-Wei Chang, Michel Galley, and Jianfeng Gao. MathVista: Evaluating mathematical reasoning  
 553 of foundation models in visual contexts. *arXiv preprint arXiv:2310.02255*, 2023a.

555 Pan Lu, Hritik Bansal, Tony Xia, Jiacheng Liu, Chunyuan Li, Hannaneh Hajishirzi, Hao Cheng,  
 556 Kai-Wei Chang, Michel Galley, and Jianfeng Gao. Mathvista: Evaluating mathematical reasoning  
 557 of foundation models in visual contexts. In *International Conference on Learning Representations*,  
 558 2023b.

559 Meta. The llama 4 herd: The beginning of a new era of natively multimodal ai innovation, April 2025.  
 560 URL <https://ai.meta.com/blog/llama-4-multimodal-intelligence/>.

562 OpenAI. Introducing OpenAI o3 and o4-mini, April 2025. URL <https://openai.com/index/introducing-o3-and-o4-mini/>.

565 Davide Paglieri, Bartłomiej Cupiał, Samuel Coward, Ulyana Piterbarg, Maciej Wolczyk, Akbir Khan,  
 566 Eduardo Pignatelli, Łukasz Kuciński, Lerrel Pinto, Rob Fergus, et al. Balrog: Benchmarking  
 567 agentic llm and vlm reasoning on games. *arXiv preprint arXiv:2411.13543*, 2024.

568 Timo Schick, Jane Dwivedi-Yu, Roberto Dessì, Roberta Raileanu, Maria Lomeli, Eric Hambro, Luke  
 569 Zettlemoyer, Nicola Cancedda, and Thomas Scialom. Toolformer: Language models can teach  
 570 themselves to use tools. *Advances in Neural Information Processing Systems*, 36:68539–68551,  
 571 2023.

573 ByteDance Seed Team. Seed1.5-VL technical report. *arXiv preprint arXiv:2505.07062*, 2025.

575 Oguzhan Topsakal, Colby Jacob Edell, and Jackson Bailey Harper. Evaluating large language models  
 576 with grid-based game competitions: an extensible llm benchmark and leaderboard. *arXiv preprint  
 577 arXiv:2407.07796*, 2024.

578 Yaoting Wang, Shengqiong Wu, Yuecheng Zhang, Shuicheng Yan, Ziwei Liu, Jiebo Luo, and Yang  
 579 Fei. Multimodal chain-of-thought reasoning: A comprehensive survey. *arXiv preprint  
 580 arXiv:2503.12605*, 2025a.

582 Ziyue Wang, Yurui Dong, Fuwen Luo, Minyuan Ruan, Zhili Cheng, Chi Chen, Peng Li, and Yang  
 583 Liu. How do multimodal large language models handle complex multimodal reasoning? placing  
 584 them in an extensible escape game. *arXiv preprint arXiv:2503.10042*, 2025b.

585 Jason Wei, Xuezhi Wang, Dale Schuurmans, Maarten Bosma, Fei Xia, Ed Chi, Quoc V Le, Denny  
 586 Zhou, et al. Chain-of-thought prompting elicits reasoning in large language models. *Advances in  
 587 neural information processing systems*, 2022.

589 Anne Wu, Kianté Brantley, and Yoav Artzi. A surprising failure? multimodal llms and the NLVR  
 590 challenge. *arXiv preprint arXiv:2402.17793*, 2024.

592 Qianqi Yan, Yue Fan, Hongquan Li, Shan Jiang, Yang Zhao, Xinze Guan, Ching-Chen Kuo, and  
 593 Xin Eric Wang. Multimodal inconsistency reasoning (mmir): A new benchmark for multimodal  
 594 reasoning models. *arXiv preprint arXiv:2502.16033*, 2025.

594 Xiang Yue, Yuansheng Ni, Kai Zhang, Tianyu Zheng, Ruoqi Liu, Ge Zhang, Samuel Stevens, Dongfu  
595 Jiang, Weiming Ren, Yuxuan Sun, et al. MMMU: A massive multi-discipline multimodal under-  
596 standing and reasoning benchmark for expert agi. In *Proceedings of the IEEE/CVF Conference on*  
597 *Computer Vision and Pattern Recognition*, 2024.

598 Di Zhang, Jingdi Lei, Junxian Li, Xunzhi Wang, Yujie Liu, Zonglin Yang, Jiatong Li, Weida Wang,  
599 Suorong Yang, Jianbo Wu, et al. Critic-V: VLM critics help catch vlm errors in multimodal  
600 reasoning. In *Proceedings of the Computer Vision and Pattern Recognition Conference*, pp.  
601 9050–9061, 2025.

602

603 Xiangxi Zheng, Linjie Li, Zhengyuan Yang, Ping Yu, Alex Jinpeng Wang, Rui Yan, Yuan Yao, and  
604 Lijuan Wang. V-mage: A game evaluation framework for assessing visual-centric capabilities in  
605 multimodal large language models. *arXiv preprint arXiv:2504.06148*, 2025.

606 Deyao Zhu, Jun Chen, Xiaoqian Shen, Xiang Li, and Mohamed Elhoseiny. MiniGPT-4: Enhancing  
607 vision-language understanding with advanced large language models. In *The Twelfth International*  
608 *Conference on Learning Representations*.

609

610 Jinguo Zhu, Weiyun Wang, Zhe Chen, Zhaoyang Liu, Shenglong Ye, Lixin Gu, Yuchen Duan, Hao  
611 Tian, Weijie Su, Jie Shao, et al. InternVL3: Exploring advanced training and test-time recipes for  
612 open-source multimodal models. *arXiv preprint arXiv:2504.10479*, 2025.

613

614

615

616

617

618

619

620

621

622

623

624

625

626

627

628

629

630

631

632

633

634

635

636

637

638

639

640

641

642

643

644

645

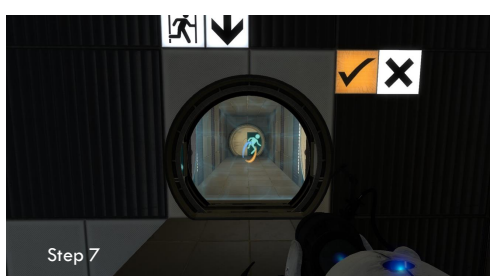
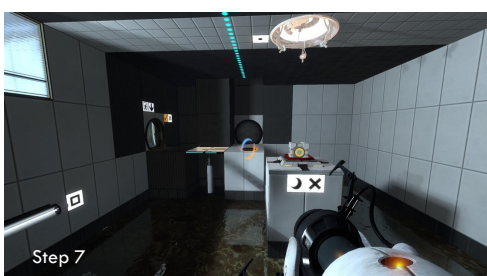
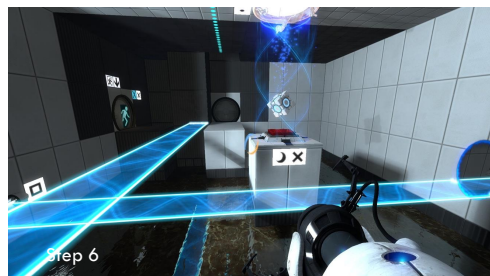
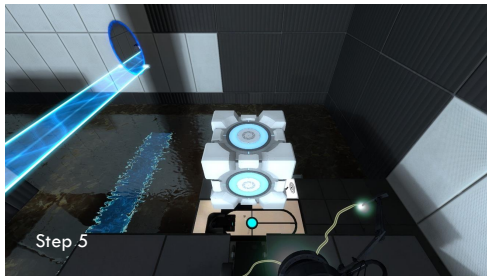
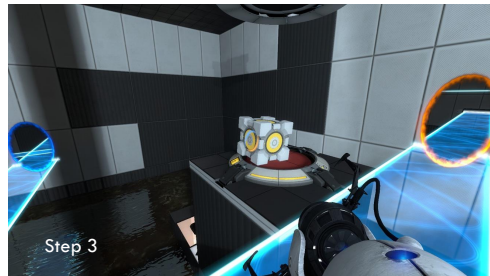
646

647

648 **A LLM USAGE STATEMENT**  
649650 Generative AI has been used to check for typos and grammatical errors in this manuscript, and to  
651 rephrase certain original sentences of the authors for correctness, conciseness and style, as they  
652 are not of English mother tongue. Any use of generative AI in this manuscript adheres to ethical  
653 guidelines for use and acknowledgment of generative AI in academic research. Each author has made  
654 a substantial contribution to the work, which has been thoroughly vetted for accuracy, and assumes  
655 responsibility for the integrity of their contributions.656  
657 **B ETHICAL STATEMENT**  
658659 As with any benchmark, there is a risk of overfitting to dataset-specific patterns. However, our setting  
660 involves abstract puzzle domains, which do not raise direct societal risks. Advancing multimodal  
661 reasoning has strong potential for positive impact in domains like healthcare, accessibility, and  
662 education. Rigorous benchmarks like MARBLE can help ensure that future systems are robust and  
663 beneficial ahead of deployment.664  
665 **C RELATED WORK**  
666667 **Chain-of-Thought and multimodal reasoning paradigms.** The Chain-of-Thought (CoT) prompting  
668 paradigm has significantly advanced reasoning in language models by enabling stepwise de-  
669 composition of complex problems (Wei et al., 2022). The Multimodal Chain-of-Thought (MCoT),  
670 its extension to the multimodal domain, represents a natural progression, encouraging models to  
671 articulate intermediate reasoning steps while integrating multiple modalities such as images, text, and  
672 diagrams. Recent works like Wang et al. (2025a) highlight prompt-based, plan-based, and learning-  
673 based MCoT strategies, yet also underscore the lack of robust, diagnostic benchmarks tailored to  
674 multimodal reasoning.675 Recent multimodal instruction tuning approaches fine-tune LLMs augmented with visual encoders  
676 to follow multimodal prompts (Li et al., 2024; Zhu et al.). While these models can generate fluent  
677 outputs, their reasoning often lacks depth or consistency, particularly on tasks involving spatial,  
678 numerical, or abstract visual patterns (Yue et al., 2024; Chia et al., 2024).679 **Multimodal reasoning benchmarks.** Several datasets have been proposed to evaluate multimodal  
680 reasoning, such as ScienceQA (Lu et al., 2022), MMMU (Yue et al., 2024), MathVista (Lu et al.,  
681 2023a), EMMA Hao et al. (2025) and MEGABench (Chen et al., 2024). These benchmarks span  
682 academic knowledge domains and require integrating visual and textual information. However, they  
683 often prioritize answer accuracy over the evaluation of the full reasoning trace, making it difficult  
684 to diagnose model errors. Others, like PuzzleVQA (Chia et al., 2024) and NLVR (Wu et al., 2024),  
685 introduce abstract reasoning challenges but are limited in modality diversity and stepwise supervision.  
686 Recent works like Critic-V Zhang et al. (2025) and MMIR Yan et al. (2025) introduced frameworks  
687 for multimodal inconsistency detection or critic-guided refinement, which improved performance but  
688 was limited to rather shallow reasoning paths.689 There are few previous benchmarking approaches that leveraged multimodal tasks inspired by  
690 video game puzzle environments (Zheng et al., 2025; Paglieri et al., 2024; Topsakal et al., 2024).  
691 Most recently and closely related, Wang et al. (2025b) proposed MM-Escape, an escape-room like  
692 environment where MLLMs have to navigate and leverage the surroundings (e.g., retrieving a hidden  
693 key) in order to escape a room. While this benchmark shares some similarity with the M-PORTAL task  
694 in MARBLE, M-PORTAL introduces a novel and much harder, multi-step problem solving challenge.  
695 To illustrate this, consider GPT-4o model which solved 70 – 100% of the maps in MM-Escape, but  
696 performed very poorly on M-PORTAL (e.g., 4.1% accuracy on fill-the-blanks).697  
698  
699  
700  
701

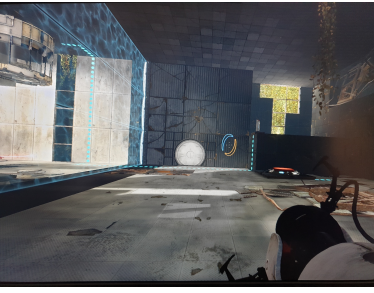
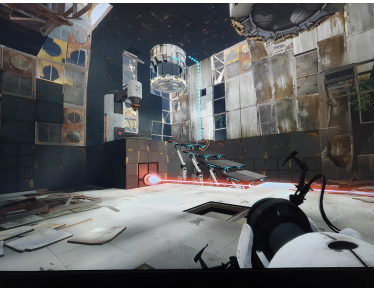
702 D ILLUSTRATION OF EXAMPLE PROBLEMS  
703704 D.1 M-PORTAL  
705706 Portal 2: Complex multi-step problem solving  
707709 Solution:  
710

711 Step 1: Place portals in positions **a**, **b** and jump down into **b** to get ejected from **a** to  
712 press the button **c**.  
713 Step 2: Button **c** releases a cube to land on button **d** which activates the bridge **e**.  
714 Step 3: Place portals in positions **f**, **g** to walk across the bridge towards the cube at  
715 location **d**.  
716 Step 4: Pick up the cube and step on button **d** which also activates the downwards  
717 pushing tractor beam at location **h**.  
718 Step 5: Throw the cube down to the device at **i** that catapults it over to the target area.  
719 Step 6: The tractor beam intercepts the cube and pushes it on the slot **j** which opens the  
720 (blue) exit door and elevates a platform at location **k**.  
721 Step 7: Place portals in positions **l**, **a**, walk across **k** to reach the exit.  
722



751 Figure 8: Overview of the Portal-2 Dataset of the MARBLE-Benchmark. Illustrated is a rather basic  
752 level Portal 2 problem, which only requires seven steps to solve. For comparison, the advanced  
753 problems introduced in this benchmark may involve several dozens of steps. Also, steps are not  
754 always decomposed into their most atomic form to keep enough complexity within a step to make  
755 mistakes harder to detect.

## Problem images (excerpt)

756  
757  
758  
759  
760  
761  
762  
763  
764765  
766  
767  
768  
769  
770  
771  
772  
773774  
775  
776  
777  
778  
779  
780  
781  
782783  
784  
785  
786  
787

## Hint image

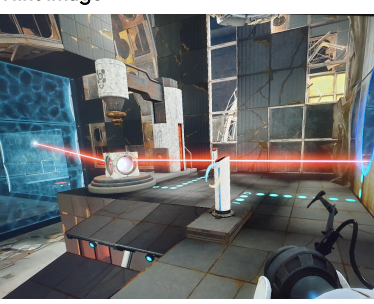
788  
789  
790  
791  
792  
793  
794  
795  
796  
797  
798799  
800  
801

Figure 9: Illustration of an example problem of the MI-PORTAL dataset (problem 5), composed of a problem description, images, solution steps, mistakes, and optional hint images.

802  
803  
804  
805  
806

Figure 8 gives an extended overview of the MI-PORTAL problem. It introduces a simple example problem, created for illustrative purposes and does not cover the full complexity the benchmark. Each map in MI-PORTAL requires a sequence of actions to solve, making it a complex multimodal reasoning problem.

807  
808  
809

Figure 9 shows a challenging example problem of the MI-PORTAL task of MARBLE. Figure 9 shows input images and instruction text that describe the problem. A manually curated solution is shown on the right side, together with five mistaken steps, below. A hint image depicts the crucial insight that allows to solve the map.

## Problem description

"You enter room 1, which is connected to room 2 on the right, separated by a shield wall. Room 1 contains a button on the floor that activates a stair leading up to a platform. On this platform, there is a switch that controls a mirror cube machine located in room 2. Room 2 features a laser source that hits the wall and a laser teleportation machine. When activated by a button press, this teleportation machine sends any object placed on it (such as a cube) to the endpoint of the laser ray, wherever the laser is directed. This allows cubes to travel through shield walls that would otherwise block movement. However, teleportation does not work through solid walls. Room 2 also has a button that activates a cube machine located next to the teleportation device. Room 3 is separated from room 1 by a shield wall and contains a button that opens the door to room 4. Room 4 is a small area with only a button on the floor, which opens the exit door."

## Solution ✓

"**Step 1:** Go to room 2 (on the right) and press the switch to drop a cube.",

"**Step 2:** Shoot a blue portal where the laser hits the wall and one on the wall that points to the central room (room 1).",

"**Step 3:** Place the cube on the laser teleportation machine and press the switch to send the cube via laser to room 1.",

"**Step 4:** Go to room 1 and place the cube on the button.",

"**Step 5:** Walk up the stairs to press the little button, which drops a mirror cube in room 1.",

"**Step 6:** Pick up the mirror cube and place it in front of the laser source such that the laser points towards room 3.",

"**Step 7:** Create a new cube by pressing the little button in room 2.",

"**Step 8:** Place the new cube on the laser teleportation machine and press the button to send the cube.",

"**Step 9:** Pick up the mirror cube and place it on the teleportation device.",

"**Step 10:** Shoot an orange portal where the laser source hits the wall and a blue portal at the wall next to the teleportation device to direct the laser to the mirror cube which needs to point to room 3.",

"**Step 11:** Activate the teleportation machine by pressing the button next to the machine.",

"**Step 12:** Go to room 3, pick one cube, and place it on the button to open the door to room 4. Take the other cube and bring it to room 4, placing it on the button on the floor to open the exit door.",

"**Step 13:** Go through the exit door. Problem solved."

## Mistakes ✗

"**Step 2:** Shoot a blue portal where the laser hits the wall and an orange portal on the same wall close to the boundary to room 1 such that the cube gets sent to room 1.",

"**Step 5:** Go to room 2 and collect the mirror cube who dropped due to the button press in room 1.",

"**Step 6:** Pick up the mirror cube and place it in front of the laser source such that the laser points towards room 2.",

"**Step 10:** Shoot an orange portal where the laser source hits the wall and a blue portal at the wall of the entrance in room 1, such that the laser points to room 3.",

"**Step 12:** Go to room 3, pick one cube, and place it on the button of room 4 to open the door in room 4. Take the other cube and placing it on the button of room 3, now both doors are open."

810 D.2 M-CUBE  
811812 Figure 10 presents a complete example question of M-CUBE task, and the solution to the instance  
813 with the corresponding 2D and 3D visualization. Figure 11 shows the prompt of the perception task.  
814

815

816

817

818

819

820

821

822

823

824

825

826

827

828

829

830

831

832

833

834

835

836

837

838

839

840

841

842

843

844

845

846

847

848

849

850

851

852

853

854

855

856

857

858

859

860

861

862

863

Happy Cube Puzzle Pieces

The figure consists of two main sections. The top section is a prompt for the Happy Cube puzzle. It shows six pieces labeled Face A through Face F, each with a 2x2 grid of squares. Edges are labeled Edge 1 (top-left), Edge 2 (top-right), Edge 3 (bottom-right), and Edge 4 (bottom-left). The prompt text provides instructions for solving the puzzle, including input requirements (six pieces with bump/gap patterns), task requirements (building a 5x5x5 cube, assigning faces, and ensuring no overlaps/gaps), and a note on corner alignment. The bottom section shows a solution to the puzzle. It includes a box for '[Thinking...]', a 'SOLUTION' box with piece assignments, a '2D Visualization' grid, and a '3D Visualization' cube. The 'SOLUTION' box contains the following assignments:

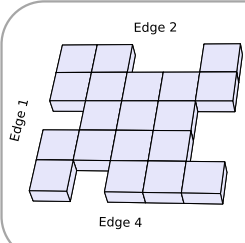
**SOLUTION**

A: (Back, 2, 1),  
B: (Bottom, 1, 2),  
C: (Top, 1, 2),  
D: (Right, 3, 2),  
E: (Left, 3, 2),  
F: (Front, 4, 3)

The 2D Visualization is a 4x4 grid of colored squares representing the cube's faces. The 3D Visualization is a 5x5x5 cube where faces are colored according to the solution.

Figure 10: Illustration of M-CUBE Problem. *Top*: Example input image and prompt of the problem. *Bottom*: Example solution to the problem (left) and corresponding 2D and 3D visualization (right). The visualization is not part of the inputs or outputs of the benchmark.

864  
865  
866  
867  
868  
869  
870  
871  
872  
873  
874



You are given an image of a  $5 \times 5$  grid. In the grid, each cell on the edges is randomly preserved or dropped, while the center  $3 \times 3$  region is always preserved. Now convert the input image into a 2D array, where 0 = gap and 1 = bump, and ensure edge1 = left, edge2 = top, edge3 = right, edge4 = bottom in the 2D array. You should answer with "Here is the converted 2D array: [array]" where [array] is a 2D array in the format of Python list of lists.

Figure 11: Prompt for evaluating the perception ability of MLLMs on M-CUBE.

875  
876  
877  
878  
879

The solution validator of M-CUBE can serve as an auxiliary tool to assist MLLM in solving the reasoning problems. Given a candidate solution, the solution validator could determine whether the solution is correct or not (binary feedback). In addition, it can also provide diagnostic information such as edge conflicts (detailed feedback). Figure 12 illustrates an example where the MLLM leverages feedback from the validator to iteratively refine its solution.

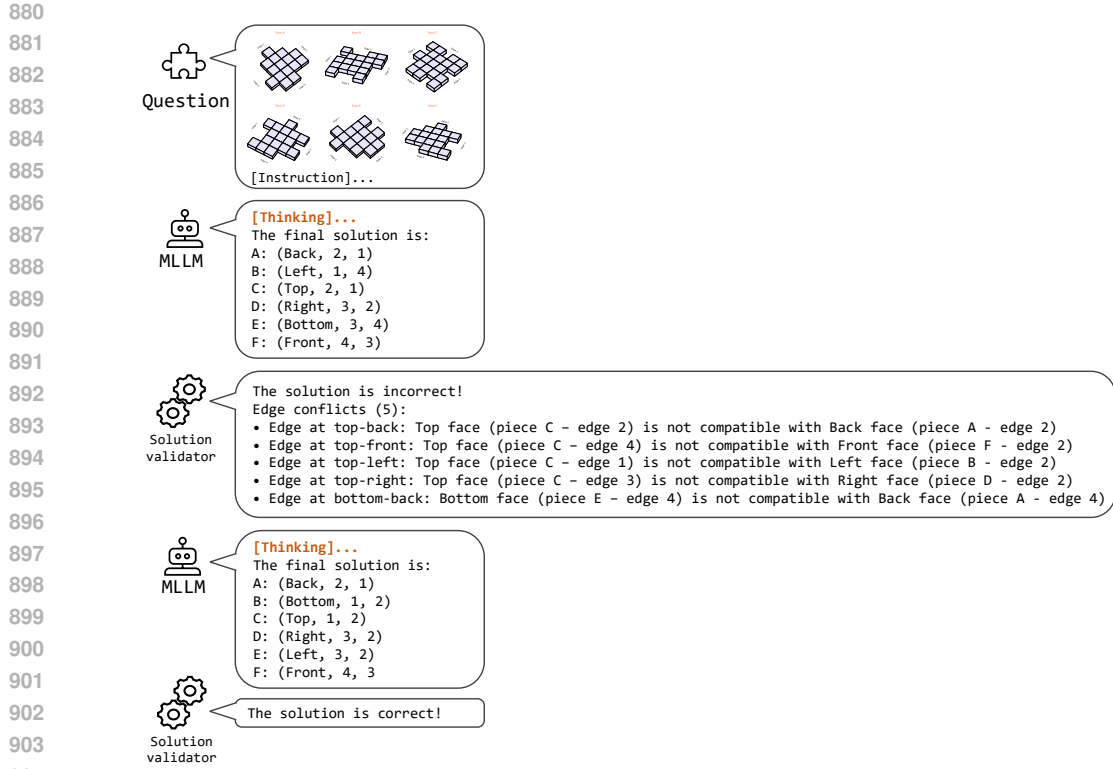


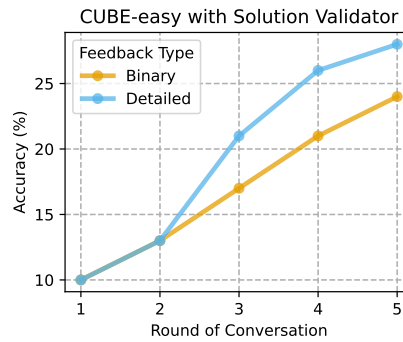
Figure 12: Example of MLLM using solution validator as a tool to gather feedback and iteratively refine its response on the M-CUBE dataset.

905  
906  
907  
908  
909  
910  
911  
912  
913  
914  
915  
916  
917

**Results with solution validator.** The ability to use tools or perform function calls has emerged as a crucial feature in latest MLLMs Schick et al. (2023). In case of M-CUBE, the solution validator could serve as an auxiliary tool to assist MLLMs in tackling complex reasoning tasks. In each round, the model proposes a candidate solution and evaluates it with the solution validator. Based on the validator's feedback, the model could iteratively refine its response towards a better solution in the next round. Specifically, we design two types of feedback: (i) Binary feedback, which simply indicates whether a solution is correct or not in a black box manner, (ii) Detailed feedback, which not only verifies the correctness of the solution but also provides diagnostic information such as which edges of the cube are in conflict. Figure 13 shows the performance of GPT-04-mini under both types of feedback. On CUBE-easy, the performance increases significantly for both binary and detailed feedback and detailed feedback consistently outperforms binary feedback, increasing

918 the performance from 10% to up to 28% accuracy after 5 rounds of interactions, which indicates the  
 919 value of diagnostic information. However, on more challenging CUBE dataset, the performance using  
 920 the solution validator tool remains 0% regardless of the feedback type, highlighting the limitation of  
 921 current MLLMs in solving harder multimodal reasoning problems.

922 In summary, we introduce a multi-step setup within M-CUBE that enables iterative refinement through  
 923 the feedback from a solution validator. This setup closely mirrors how humans tackles real-world  
 924 problem-by making initial attempts, gathering feedback from the environment, and refining their  
 925 strategies accordingly. However, many current reasoning models would not retain and build upon  
 926 previous reasoning steps, often discarding the reasoning in earlier context<sup>1</sup>, resulting in less effective  
 927 reasoning in multi-round setup. Therefore, future models capable of interleaved thinking and tool use  
 928 would benefit more from such validator-assisted setup.



<sup>1</sup>Check this OpenAI API document for example.

972 D.3 M-MAZE  
973974 Figure 14 presents an example question of M-MAZE.  
975976 **Labyrinth Puzzles – Easy**977 You are a spatial-planning assistant that plays Labyrinth from  
978 arbitrary board states.979 **INPUT**

980 You will be given the current game observation:  
 981 - Phase: one of {INSERT, MOVE} indicating which action you  
 982 must take now.  
 983 - Board (7x7): each tile has corridors/walls (shape in {I, L, T})  
 984 plus rotation in {0, 1, 2, 3}), indexed 0..6 on both axes.  
 985 - Objects grid (size x size): a Python list of lists of strings (letters  
 986 or '-' for empty) indicating item placement.  
 987 - Extra tile: the tile currently out of the board (with  
 988 shape/rotation), encoded by a token (see conventions below).  
 989 - Player position: (x,y) of our player, 0-based.  
 990 - Target: a treasure object represented by its name mapped to a  
 991 letter (A–X) in symbolic representation.  
 992 - Visual encoding: the player is a green circular pawn labeled  
 993 "P1"; the target is a black icon of the object.  
 994 - Right-side panel on the image: shows "Extra Tile" and "Target"  
 995 sections with the current extra tile and the target.  
 996 - last\_insert: the previous insertion, if any, as (side, slot); used  
 997 to enforce the "no immediate reversal" rule.

998 **TASK**

999 Propose a complete multi-turn plan at once. Each turn consists  
 1000 of INSERT then MOVE. Aim to reach the Target as soon as  
 1001 possible.  
 1002 Include only the turns necessary to reach the target; stop at  
 1003 success (no extra turns).

1004 **RULES**

1005 **Phase = INSERT** (must happen before any move each turn):  
 1006 - Set the loose tile to the specified rotation (see tile  
 1007 conventions below), then insert it from side into slot.  
 1008 - This shifts that entire row/column by one; the opposite edge  
 1009 tile is ejected and becomes the new loose tile.  
 1010 - Direction→ejection: Left inserts eject Right edge; Right ejects  
 1011 Left; Top ejects Bottom; Bottom ejects Top.  
 1012 - Objects behavior: treasures/items stay attached to their  
 1013 tiles; they shift with the row/column and if on the ejected tile,  
 1014 they leave the board (no wrap) and only re-enter if that tile is  
 1015 later re-inserted.  
 1016 - Any pawns on that line shift with the tiles; if pushed off, they  
 1017 wrap to the newly inserted tile on the opposite edge.  
 1018 - No immediate reversal: you cannot insert from the opposite  
 1019 side into the same slot as last\_insert.  
 1020 - After inserting, the environment will switch to Phase = MOVE.  
 1021

1022 **Phase = MOVE**:

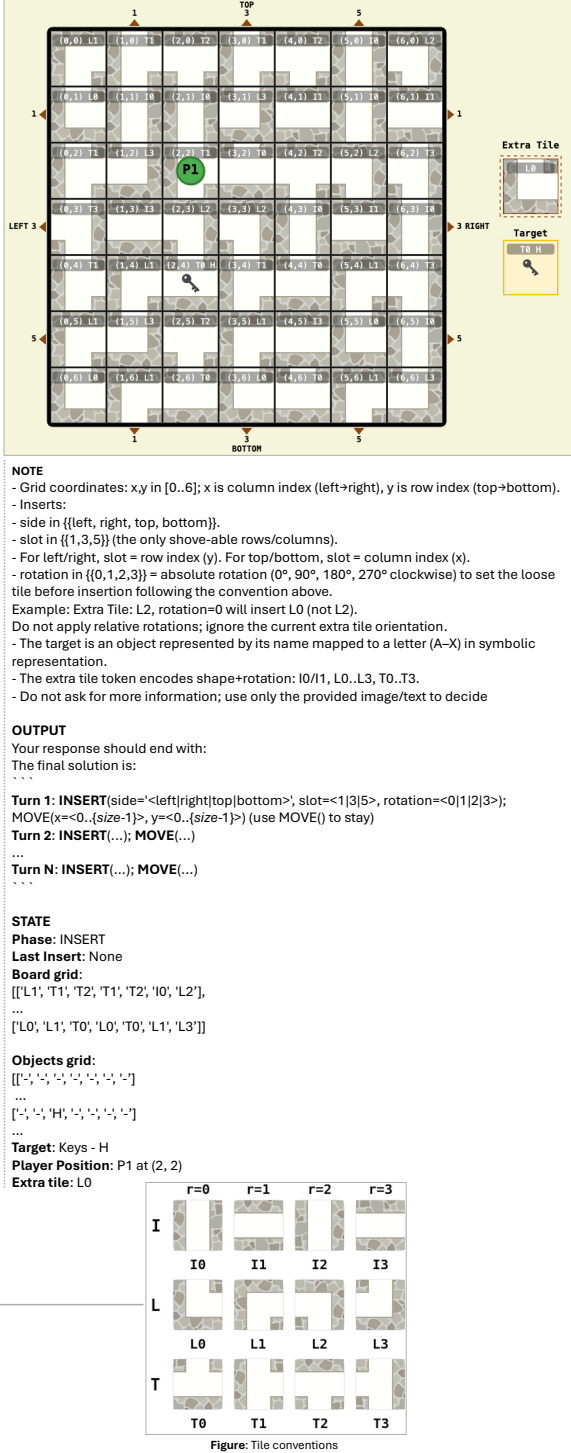
1023 - Move your pawn along open corridors to any reachable cell  
 1024 (unlimited distance along connected paths).  
 1025 - Adjacency rule: a step to an orthogonal neighbor is legal only  
 1026 if both tiles open toward each other (N/S, S/N, E/W, W/E).  
 1027 - To stay, output MOVE(); the keyword is required (not optional).  
 1028 - After moving, the environment will switch to Phase = INSERT  
 1029 (next turn) or declare success if the Target is reached.

1030 **Tile/token convention for Extra**

1031 - Shapes: I (straight corridor), L (corner/bend), T (three-way  
 1032 junction).  
 1033 - Openings are on North (up), East (right), South (down), West  
 1034 (left).  
 1035 - Rotation is clockwise; board top is North.

1036 **Visual Descriptions:**

1037 - I (straight): A corridor connecting two opposite sides  
 1038 \* I0 = vertical corridor (connects top↔bottom, North↔South)  
 1039 \* I1 = horizontal corridor (connects left↔right, East↔West)  
 1040 \* I2=I0, I3=I1 (same visual appearance). Prefer I0/I1.  
 1041  
 1042 - L (corner): A bent corridor connecting two adjacent sides  
 1043 \* L0 = connects top+right (North+East)  
 1044 \* L1 = connects right+bottom (East+South)  
 1045 \* L2 = connects bottom+left (South+West)  
 1046 \* L3 = connects left+top (West+North)  
 1047  
 1048 - T (junction): A corridor with three openings  
 1049 \* T0 = opens to top+left+right (North+East+West)  
 1050 \* T1 = opens to right+bottom+top (East+South+North)  
 1051 \* T2 = opens to bottom+left+right (South+West+East)  
 1052 \* T3 = opens to left+top+bottom (West+North+South)

1023 Figure 14: Illustration of M-MAZE Problem: Example input image and prompt of the problem in  
1024 Visual Harness + Symbolic Representation setting.  
1025

1026

1027

1028

1029

1030

1031

1032

1033

1034

1035

1036

1037

1038

1039

1040

1041

1042

1043

1044

1045

1046

1047

1048

1049

1050

1051

1052

1053

1054

1055

1056

1057

1058

1059

1060

1061

1062

1063

1064

1065

1066

1067

1068

1069

1070

1071

1072

1073

1074

1075

1076

1077

1078

1079

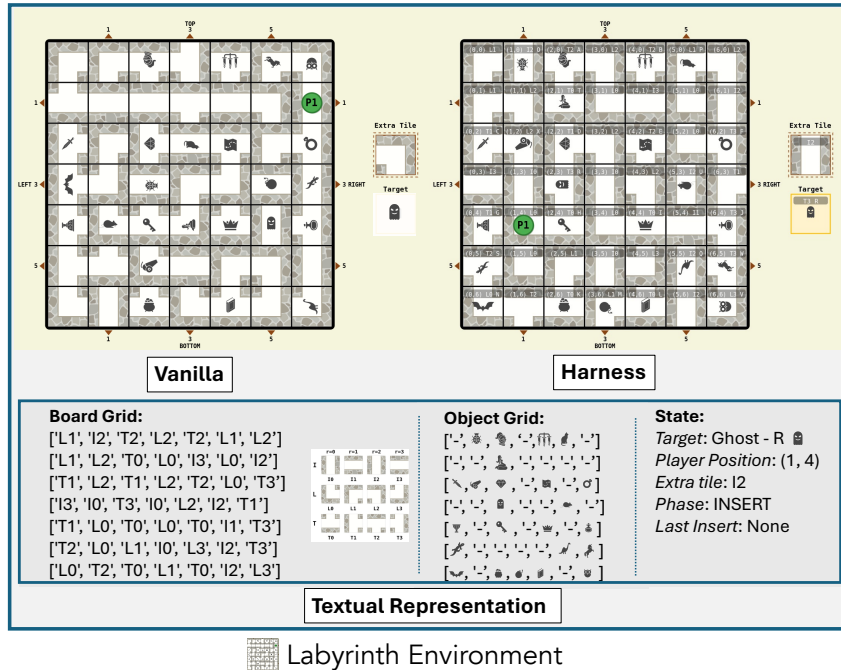


Figure 15: Overview of the M-MAZE board representation. **Visual Only** corresponds to the *Vanilla* setting where only the board image along selected textual game informations (*Phase*, *target*) are given. **Visual Harness** adds an overlay of the coordinates on each tile (with respect to the *Vanilla* setting). **Symbolic/Textual representation** adds the *board grid* and *object grid* as arrays in the prompt thereby reducing the required visual parsing capabilities required by the models.

1080 E EXPERIMENT DETAILS.  
10811082 Table 3 provides a comprehensive list of all the models evaluated in this paper, along with the  
1083 hyperparameters. We use the same hyperparameters for evaluating both the M-PORTAL and M-CUBE  
1084 tasks. For open-source models such as Qwen2.5-VL-72B, InternVL3-78B and Llama-4-Scout, we  
1085 use vLLM Kwon et al. (2023) for efficient inference, with a setting of temperature of 0 and maximum  
1086 output token length of 16,000 for all the models. The open-source models are evaluated on the whole  
1087 evaluation suite of M-CUBE and M-PORTAL.1088 In contrast, close-source models such as GPT-4o, Claude-3.7-Sonnet, Gemini-2.5-pro, GPT-o3 and  
1089 GPT-4o-mini are evaluated with their respective APIs. The "reasoning effort" parameter, which  
1090 controls the allowed length of reasoning chain, is set to "medium" for GPT-4o-mini and Gemini-2.5-  
1091 Pro, and 12,000 for Claude-3.7 Sonnet. Due to the limit of budget, we choose 200 representative  
1092 examples on M-CUBE and M-MAZE. The whole set of M-PORTAL is used for evaluating close-  
1093 source models.1094  
1095 Table 3: MLLMs and corresponding hyperparameters for evaluating MARBLE benchmark. "Rea-  
1096 soning effort" represents the budget of reasoning tokens to generate before the final response. \* For  
1097 reasoning models, max tokens denote the sum of tokens generated for reasoning and final response.  
1098

Model	Date	Temperature	Reasoning Effort	Max Tokens <sup>*</sup>
Qwen2.5-VL-72B	2025.02.19	0.0	-	16,000
InternVL3-78B	2025.04.11	0.0	-	16,000
Llama-4-Scout	2025.04.05	0.0	-	16,000
Qwen3-235B-A22B	2025.04.29	0.6	-	16,000
GPT-4o	2024.08.06	0.0	-	16,000
DeepSeek-R1	2025.01.22	-	-	16,000
DeepSeek-R1-0528	2025.05.28	-	-	16,000
Seed-1.5-VL	2025.04.28	-	-	16,000
Claude-3.7-Sonnet	2025.02.19	-	12,000	16,000
Gemini-2.5-pro	2025.05.06	-	medium	25,000
GPT-o4-mini	2025.04.16	-	medium	25,000
GPT-o3	2025.04.16	-	medium	40,000
GPT-5	2025.08.07	-	medium	40,000
Grok 4	2025.07.09	0.0	-	25,000

## F ADDITIONAL RESULTS

## F.1 COST/TOKEN USAGE

Model	Input \$ / 1M	Output \$ / 1M	M-PORTAL			M-CUBE			M-MAZE		
	In	Out	Total \$	In	Out	Total \$	In	Out	Total \$	In	Out
<i>OpenAI</i>											
GPT-5	1.25	10.00	0.74	14.97	15.71	0.33	4.99	5.32	0.46	12.98	13.44
o4-mini	1.10	4.40	0.90	1.36	2.26	0.66	1.38	2.04	0.69	6.31	7.00
o3	2.00	8.00	1.24	5.77	7.00	0.56	2.97	3.52	0.76	16.10	16.86
<i>Anthropic</i>											
Claude 3.7 Sonnet	3.00	15.00	2.16	5.76	7.92	1.23	39.52	40.74	1.92	36.92	38.84
<i>Google</i>											
Gemini 2.5 Pro	1.25	10.00	0.85	1.77	2.63	0.18	16.77	16.95	0.40	29.96	30.36
Gemini 2.5 Flash	0.30	2.50	0.21	2.21	2.42	0.04	3.96	4.00	0.10	6.22	6.32
<i>DeepSeek</i>											
DeepSeek-R1-250528	0.56	2.25	0.12	5.08	5.20	0.10	9.59	9.69	0.19	7.11	7.30
<i>Seed / Doubao</i>											
Seed 1.5 VL	0.42	1.26	0.29	0.39	0.68	0.15	0.98	1.13	0.22	1.13	1.35
<i>xAI</i>											
Grok-4	3.00	15.00	2.03	78.32	80.35	1.33	41.14	42.46	1.92	60.66	62.58
Grok-4 Fast	0.20	0.50	0.15	1.57	1.71	0.03	0.22	0.25	0.10	0.34	0.44

Table 4: Total inference costs by task ( $N = 200$ ).

Model	M-PORTAL		M-CUBE		M-MAZE	
	In	Out	In	Out	In	Out
<i>OpenAI</i>						
GPT-5	2.96	7.49	1.32	2.50	1.84	6.49
o4-mini	4.09	1.55	3.00	1.57	3.14	7.17
o3	3.10	3.61	1.40	1.86	1.90	10.06
<i>Anthropic</i>						
Claude 3.7 Sonnet	3.60	1.92	2.05	13.17	3.20	12.31
<i>Google</i>						
Gemini 2.5 Pro	3.40	0.89	0.72	8.38	1.60	14.98
Gemini 2.5 Flash	3.50	4.42	0.67	7.92	1.67	12.44
<i>DeepSeek</i>						
DeepSeek-R1	1.07	11.29	0.89	21.31	1.70	15.80
<i>Seed / Doubao</i>						
Seed 1.5 VL	3.45	1.55	1.79	3.89	2.62	4.48
<i>xAI</i>						
Grok-4	3.38	26.11	2.22	13.71	3.20	20.22
Grok-4 Fast	3.75	15.70	0.75	2.20	2.50	3.40

Table 5: Average Token Usage per puzzle (in thousands) per task ( $N = 200$ ).

## F.2 CONFIDENCE INTERVAL OF HUMAN EVALUATION

Table 6: Performance of human (mean  $\pm$  std) on all the tasks of MARBLE.

Models	M-PORTAL		M-CUBE		M-MAZE	
	Binary	Blanks	CUBE	CUBE-easy	MAZE	MAZE-easy
Human	-	$37.5 \pm 22.2$	$0.0 \pm 0.0$	$85.0 \pm 12.2$	$55.0 \pm 7.1$	$80.0 \pm 14.1$

1188 F.3 PERCEPTION

1189

## 1190 F.3.1 BOARD PARSING

1191

1192

1193

1194

1195

1196

1197

1198

1199

1200

1201

1202

## Board Parsing

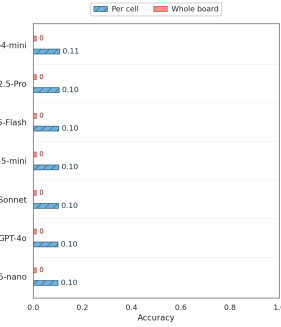
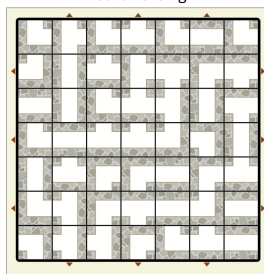


Figure 16: **Perception is also a bottleneck for M-MAZE.** *Left:* Similar to 5, board parsing is a perception task designed to test MLLM’s ability on retrieve structured information from visual input and example response of an MLLM. *Right:* Performance of 7 MLLMs on this perception task based on 200 test examples. Accuracy is measured both at individual cells and for the entire  $7 \times 7$  board. All the MLLMs perform poorly and completely fail on the whole-board accuracy. \* we modify the prompt for readability and avoid redundancy with earlier sections

## F.3.2 GAMESTATE PARSING

1209

1210

1211

1212

1213

1214

1215

1216

1217

1218

1219

1220

1221

## GameState Parsing

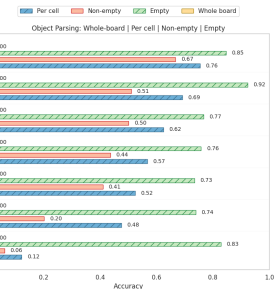
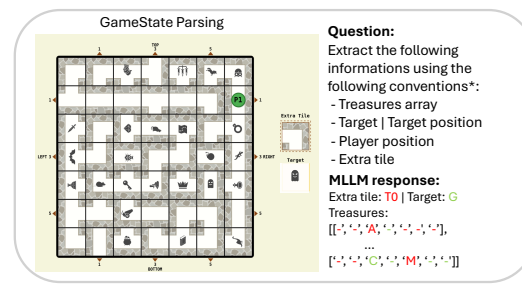


Figure 17: *Left:* GameState parsing task testing MLLMs’ ability to extract structured information (treasures array, target and position, player position, extra tile) from visual board input (full prompt in Appendix) and example MLLM response. *Right:* Performance of 7 MLLMs on this perception task based on 200 test examples. Accuracy measured at individual cells (per cell, non-empty, empty) and for the entire board. All MLLMs perform poorly and completely fail on whole-board accuracy. \* we modify the prompt for readability and avoid redundancy with earlier sections

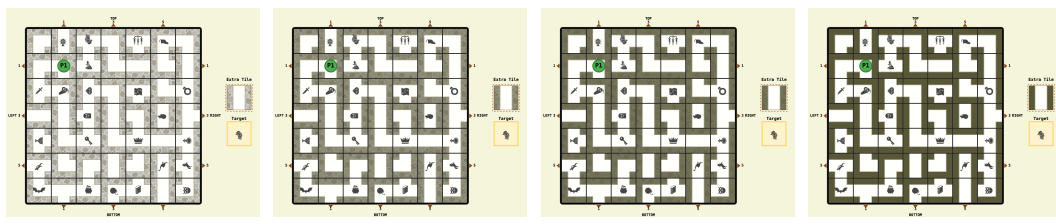
## F.3.3 OPAQUE ABLATION

1228

1229

1230

1231



1232

1233

1234

1235

1236

1237

1238

1239

1240

1241

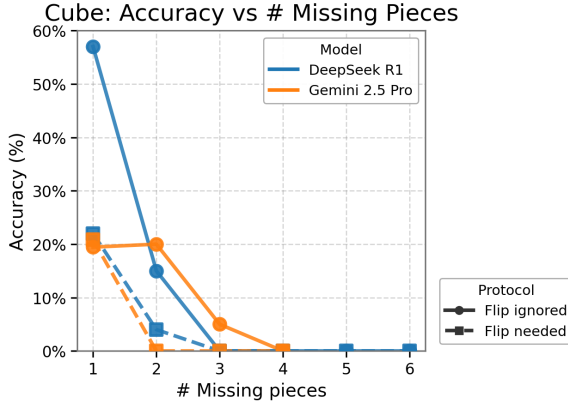
Figure 18: Visual ablation on M-MAZE across varying texture opacity levels.

1242 Table 7: Opacity Sweep on **MAZE** task on **GPT-5-mini** with  $D=0$  and oracle perception (Visual  
 1243 Harness + Symbolic).

Model	$O = 0.0$	$O = 0.2$	$O = 0.5$	$O = 0.8$	$O = 1.0$
GPT-5-mini	0.19	0.22	0.17	0.21	0.14

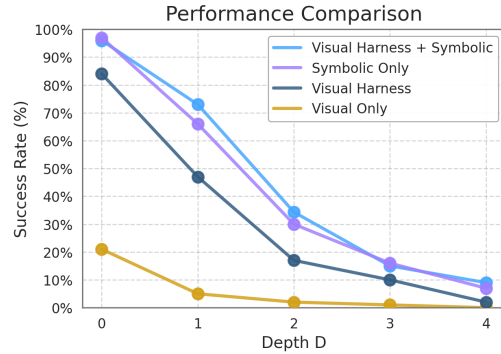
#### F.4 ISOLATING PERCEPTION FROM PLANNING DIFFICULTY.

##### F.4.1 M-CUBE

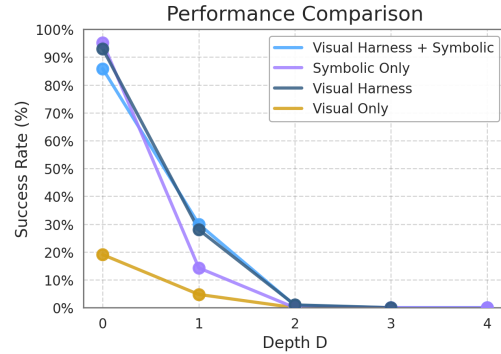


1266 Figure 19: Performance of **DeepSeek R1** & **Gemini 2.5 Pro** across varying levels of task difficulty  
 1267 of the M-CUBE dataset ( $F=P$ ) | Symbolic representation

##### F.4.2 M-MAZE



1284 Figure 20: Success rate (%) of GPT-5-mini  
 1285 on MAZE using different visual settings across  
 1286 depths.



1284 Figure 21: Success rate (%) of Gemini 2.5 Flash  
 1285 on MAZE using different visual settings across  
 1286 depths

1296 F.5 INTERMEDIATE SUCCESS METRICS.  
12971298 F.5.1  M-CUBE  
12991300 For M-CUBE, we have the following additional metrics:  
1301

- **Edit distance to GT (↓):** Per-sample distance over 6 pieces comparing (face, left-edge, top-edge); range 0–18. Normalized =  $\frac{\text{distance}}{18}$ .
- **Correct faces (↑):** Pieces placed on the correct cube face, ignoring rotation; range 0–6. Ratio =  $\frac{\text{value}}{6}$ .
- **Rotation correct (↑):** Among face-correct pieces, fraction with correct (left-edge, top-edge) orientation.
- **Connectivity violations (↓):** Count of adjacent face-edge pairs that fail to interlock when assembled; range 0–12 (12 total adjacencies).

1310 Table 8:  M-CUBE- Intermediate Success Metrics  
1311

1312 Model	1313 Edit Dist. (↓)	1314 Correct Faces (↑)	1315 Connectivity Violations (↓)
1316  Claude Sonnet 3.7	14.00	1.18	8.62
1317  DeepSeek R1	13.73	1.07	8.98
1318  Seed 1.5 VL	14.07	0.95	5.54
1319  Gemini 2.5 Flash	14.04	0.96	9.80
1320  Gemini 2.5 Pro	14.14	0.81	10.08
1321  GPT 4o	14.10	1.20	10.20
1322  GPT 5	13.78	0.78	6.89
1323  Grok 4 0709	13.93	1.13	9.79
1324  Grok 4 Fast Reasoning	14.12	1.00	7.47
1325  InternVL3 78B	14.10	0.98	1.94
1326  Llama 4 Scout 17B 16E Instruct	14.17	0.84	3.96
1327  o3	13.69	1.18	5.46
1328  o4-mini	13.92	0.99	3.74
1329  Qwen2.5 VL 72B Instruct	13.94	1.07	9.78
1330  Qwen3 235B A22B	14.07	0.95	8.26

1332 F.5.2  M-MAZE  
13331334 For M-MAZE, we have the following additional metrics:  
1335

- **Turn closeness (↑):** At step  $t$ , defined as  $c_t = 1 - \frac{m_t}{m_0}$ , where  $m_t$  is the minimal turns-to-go from the current state and  $m_0$  is that value at the start. We report  $\max_t c_t$  across the trajectory, i.e., the best normalized progress toward the goal.

1339  
1340  
1341  
1342  
1343  
1344  
1345  
1346  
1347  
1348  
1349

1350  
1351  
1352  
1353  
1354  
1355  
1356  
1357  
1358  
1359  
1360  
1361  
1362  
1363  
1364  
1365  
1366  
1367  
1368  
1369  
1370

Model	Turn Closeness ( $\uparrow$ )	Plan Length	Turn Distance
Claude Sonnet 3.7	0.22 $\pm$ 0.26	1.52 $\pm$ 1.18	1.77 $\pm$ 0.71
DeepSeek R1	0.24 $\pm$ 0.27	1.83 $\pm$ 0.71	1.73 $\pm$ 0.71
DeepSeek V3	0.33 $\pm$ 0.38	1.53 $\pm$ 1.06	1.45 $\pm$ 0.90
Seed 1.5 VL	0.15 $\pm$ 0.23	1.30 $\pm$ 0.70	1.92 $\pm$ 0.65
Gemini 2.5 Flash	0.14 $\pm$ 0.23	1.07 $\pm$ 0.54	1.90 $\pm$ 0.64
Gemini 2.5 Pro	0.34 $\pm$ 0.39	1.50 $\pm$ 0.59	1.47 $\pm$ 0.94
GPT 4o	0.14 $\pm$ 0.25	1.61 $\pm$ 0.79	1.90 $\pm$ 0.70
GPT 5	0.72 $\pm$ 0.41	1.89 $\pm$ 0.74	0.63 $\pm$ 0.93
GPT 5 mini	0.64 $\pm$ 0.39	3.71 $\pm$ 1.75	0.99 $\pm$ 0.98
GPT 5 nano	0.38 $\pm$ 0.35	3.61 $\pm$ 1.78	1.54 $\pm$ 0.86
Grok 4 0709	0.52 $\pm$ 0.48	1.50 $\pm$ 1.39	1.02 $\pm$ 1.01
Grok 4 Fast Reasoning	0.82 $\pm$ 0.34	2.54 $\pm$ 1.09	0.41 $\pm$ 0.81
o3	0.74 $\pm$ 0.42	2.05 $\pm$ 1.27	0.55 $\pm$ 0.90

Table 9:  M-MAZE Easy - Intermediate Success Metrics

1371  
1372  
1373  
1374  
1375  
1376  
1377  
1378  
1379  
1380  
1381

Model	Turn Closeness ( $\uparrow$ )	Plan Length	Turn Distance
Claude Sonnet 3.7	0.27 $\pm$ 0.17	2.15 $\pm$ 1.97	2.86 $\pm$ 0.38
DeepSeek R1	0.34 $\pm$ 0.15	2.00 $\pm$ 0.90	2.62 $\pm$ 0.51
Seed 1.5 VL	0.27 $\pm$ 0.07	1.18 $\pm$ 0.59	2.92 $\pm$ 0.27
Gemini 2.5 Flash	0.26 $\pm$ 0.11	1.69 $\pm$ 5.72	2.92 $\pm$ 0.27
Gemini 2.5 Pro	0.28 $\pm$ 0.08	1.09 $\pm$ 0.29	2.90 $\pm$ 0.30
GPT 4o	0.27 $\pm$ 0.06	1.42 $\pm$ 0.55	2.94 $\pm$ 0.24
GPT 5	0.29 $\pm$ 0.10	1.72 $\pm$ 1.43	2.88 $\pm$ 0.33
GPT 5 mini	0.42 $\pm$ 0.23	3.68 $\pm$ 2.10	2.47 $\pm$ 0.81
GPT 5 nano	0.46 $\pm$ 0.21	4.32 $\pm$ 1.92	2.34 $\pm$ 0.78
Grok 4 0709	0.21 $\pm$ 0.14	1.21 $\pm$ 0.90	2.92 $\pm$ 0.27
Grok 4 Fast Reasoning	0.28 $\pm$ 0.08	1.49 $\pm$ 0.59	2.88 $\pm$ 0.33
o3	0.20 $\pm$ 0.15	1.00 $\pm$ 0.93	2.93 $\pm$ 0.29
o4-mini	0.40 $\pm$ 0.20	3.49 $\pm$ 1.37	2.55 $\pm$ 0.77

Table 10:  M-MAZE- Intermediate Success Metrics

1398  
1399  
1400  
1401  
1402  
1403

1404  
1405

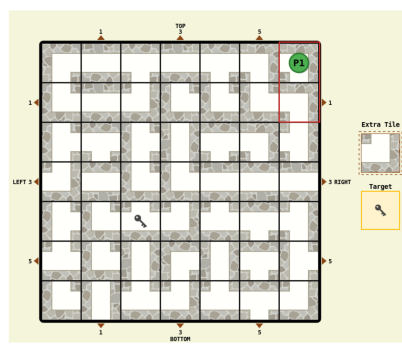
## F.6 ERROR ANALYSIS

1406  
1407  
1408  
1409  
1410

To strengthen the insights drawn from MARBLE, as suggested by reviewers, we categorized model errors across all three tasks. Specifically, we employed a **human-in-the-loop multi-label classification** approach, using experienced players of the respective tasks as annotators, to provide a fine-grained analysis of model capabilities. We report detailed error proportions below. This analysis focuses on **Claude Sonnet 3.7 & Gemini 2.5 Pro** which expose their reasoning traces.

1411  
1412F.6.1  M-MAZE1413  
1414

## Adjacency Error

1415  
1416  
1417  
1418  
1419  
1420  
1421  
1422  
1423  
1424  
1425  
1426

The current player P1 is at (6, 0). The target 'H' (Keys) is at (2, 4). The extra tile is L3.

First, let's determine if there's a path from P1's current position to the target.

Let's trace a path:

1. **P1 at (6,0) L2 (S-W)**: Can move South to (6,1) or West to (5,0). Let's try going South.
  - \* (6,0) L2 has a South opening.
2. **(6,1) L2 (S-W)**: (6,1) L2 has a North opening (connecting to (6,0)) and a South opening. Can move South to (6,2).
3. **(6,2) T3 (N-W-S)**: (6,2) T3 has a North opening (connecting to (6,1)) and a South opening. Can move South to (6,3).

4. **(6,3) I3 (E-W)**: (6,3) I3 has a North opening (connecting to (6,2)) and a West opening. Can move West to (5,3).

\* (6,3) I3 has a North opening, so it connects to (6,2) T3's South opening. This is valid.

5. **(5,3) I1 (E-W)**: (5,3) I1 has an East opening (connecting to (6,3)) and a West opening. Can move West to (4,3).

6. **(4,3) I3 (E-W)**: (4,3) I3 has an East opening (connecting to (5,3)) and a West opening. Can move West to (3,3).

7. **(3,3) L0 (N-E)**: (3,3) L0 has an East opening (connecting to (4,3)) and a West opening. Can move West to (2,3).

8. **(2,3) L0 (N-E)**: (2,3) L0 has an East opening (connecting to (3,3)) and a South opening. Can move South to (2,4).

\* (2,3) L0 has a North opening, so it connects to (3,3) L0's West opening. This is valid.

9. **(2,4) T0 (N-E-W)**: (2,4) T0 has a North opening (connecting to (2,3)). This is the target tile.

All connections along this path are valid. Therefore, P1 can reach the target (2,4) without any board modifications.

However, the game rules require an 'INSERT' action before any 'MOVE' action in each turn.

Since this is the first turn, we must perform an insertion. The goal is to reach the target as soon as possible, so we should choose an insertion that does not break the existing path.

The path uses the following cells:

(6,0), (6,1), (6,2), (6,3), (5,3), (4,3), (3,3), (2,3), (2,4).

Shove-able rows are 1, 3, 5.

Shove-able columns are 1, 3, 5.

Let's analyze the impact of inserting into these slots:

\* **Row 1\*\***: Affects (x,1) tiles. The path uses (6,1). If row 1 is shifted, (6,1) will change, potentially breaking the (6,0)-(6,1)-(6,2) connection.

\* **Row 3\*\***: Affects (x,3) tiles. The path uses (6,3), (5,3), (4,3), (3,3), (2,3). Shifting this row would definitely break the path.

\* **Row 5\*\***: Affects (x,5) tiles. The path does not use any tiles in row 5. Inserting into row 5 will not affect the path.

\* **Column 1\*\***: Affects (1,y) tiles. The path does not use any tiles in column 1. Inserting into column 1 will not affect the path.

\* **Column 3\*\***: Affects (3,y) tiles. The path uses (3,3). Shifting this column would definitely break the path.

\* **Column 5\*\***: Affects (5,y) tiles. The path uses (5,3). Shifting this column would definitely break the path.

To ensure the path remains intact, we must insert into either row 5 or column 1. Let's choose to insert into row 5.

The extra tile is L3. We can rotate it to any orientation (0, 1, 2, 3).

Since the specific rotation doesn't matter for preserving the path in row 5, we can choose 'rotation=0'. L3 with rotation 0 becomes L0 (N-E). So, the plan is to insert the extra tile into row 5 from the left side, then move P1 to the target.

The final solution is:

...

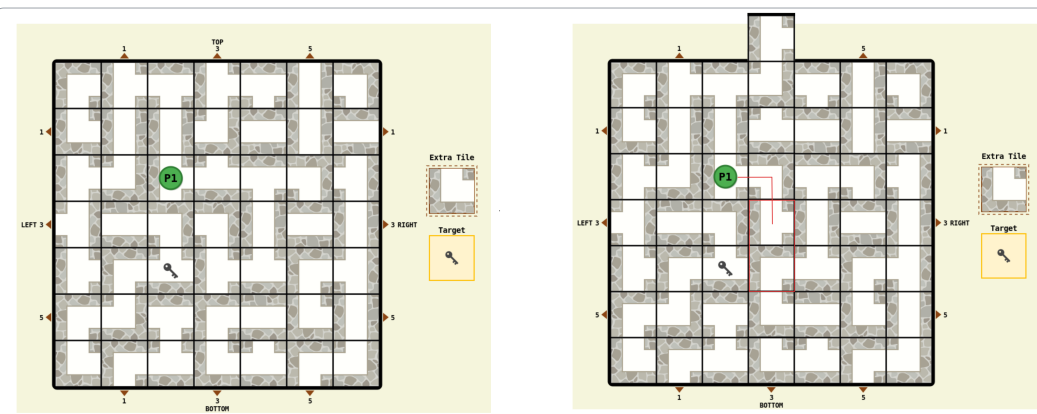
Turn 1: INSERT(side='left', slot=5, rotation=0); MOVE(x=2, y=4)

1454  
1455  
1456  
1457

Figure 22: A reasoning trace from  Gemini 2.5 Flash on the  MI-MAZE task, demonstrating a critical **adjacency error**. Although the model attempts to trace a path, it incorrectly assumes that two tiles are connected, failing to properly verify the tile openings. This misinterpretation of the board state leads it to find an invalid path, a common failure mode for models on this task.

1458  
1459

## State-Update Error

1460  
1461  
1462  
1463  
1464  
1465  
1466  
1467  
1468  
1469  
1470  
1471  
14721473  
1474  
1475  
1476  
1477  
1478  
1479  
1480  
1481  
1482  
1483  
1484  
1485  
1486  
1487  
1488  
1489  
1490  
1491  
1492  
1493  
1494  
1495  
1496  
1497  
1498  
1499  
1500  
1501  
1502  
1503  
1504  
1505  
1506  
1507  
1508  
1509  
1510  
1511

INSERT(side='bottom', slot=3, rotation=0)

### Analysis for Reaching Target 'H' at (2,4)

The player starts at (2,2), and the target treasure 'H' is located at (2,4). The key issue is the lack of a direct vertical path due to mismatched openings between:

- \*\*Player tile (2,2)\*\*: 'T1' (opens north, east, south).
- \*\*Adjacent tile (2,3)\*\*: 'L2' (opens south and west; no north opening to receive south from (2,2)).

### Plan

We will shift column 3 (valid slot=3) from the \*\*bottom\*\* to force tile 'T2' (with west opening) into position (3,4), creating a horizontal connection between (3,4) and target (2,4). Steps:

1. \*\*Insertion\*\*: Insert extra tile (L0) with rotation=0 into column 3 from the bottom. This:

- Shifts column 3 upward.
- Moves 'T2' (opens bottom, left, right) into (3,4), which now connects west to target (2,4) (east opening).
- Leaves player/target tiles unchanged (column 2 unaffected).
- New extra tile is ejected from column 3's top.

2. \*\*Movement Path\*\*: After insertion, the board has a connected route:

- (2,2) → East to (3,2):  
'T1' (east) connects to 'L2' (west) at (3,2).
- (3,2) → South to (3,3):  
'L2' (south) connects to 'T1' (north) at (3,3).
- (3,3) → East to (3,4):  
'T1' (east) connects to 'T2' (west) at (3,4).
- (3,4) → West to (2,4):  
'T2' (west) connects to 'T0' (east) at target (2,4).

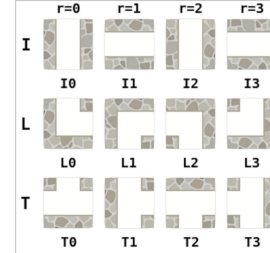
### Solution

``

The final solution is:

Turn 1: INSERT(side='bottom', slot=3, rotation=0); MOVE(2,4)

``



1512    **Legality Errors** .  
1513

1514

1515

1516

1517    Turn 1: INSERT(side='right', slot=5, rotation=0); MOVE(x=5, y=4)

1518    Turn 2: INSERT(side='top', slot=5, rotation=2); MOVE()

1519    Turn 3: INSERT(side='left', slot=3, rotation=1); MOVE(x=4, y=3)

1520    Turn 4: INSERT(side='bottom', slot=3, rotation=0); MOVE(x=3, y=3)

1521    Turn 5: MOVE(x=2, y=3)

1522    Turn 6: MOVE(x=2, y=2)

1523    Turn 7: MOVE(x=2, y=1)

1524    Turn 8: MOVE(x=2, y=0)

1525

1526

1527

1528    The final solution is:

1529    ``

1530    Turn 1: INSERT(side='right', slot=5, rotation=0); MOVE(x=5, y=4)

1531    Turn 2: INSERT(side='top', slot=5, rotation=2); MOVE()

1532    Turn 3: INSERT(side='left', slot=3, rotation=1); MOVE(x=4, y=3)

1533    Turn 4: INSERT(side='bottom', slot=3, rotation=0); MOVE(x=3, y=3)

1534    Turn 5: MOVE(x=2, y=3)

1535    Turn 6: MOVE(x=2, y=2)

1536    Turn 7: MOVE(x=2, y=1)

1537    Turn 8: MOVE(x=2, y=0)

1538    ``

1539

1540

1541

1542

1543

1544    The final solution is:

1545    ``

1546    Turn 1: INSERT(side='top', slot=6, rotation=0); MOVE(x=6, y=3)

1547    ``

1548

1549

1550    Figure 24: Examples of **Insert Legality Errors** on the  M-MAZE task. The top plan (from  GPT-5-mini) shows illegal turns (e.g., 5-8) that only contain a MOVE action, violating the rule that  
1551    every turn must have an INSERT. The bottom plan (from  Qwen2.5 VL 72B) shows an INSERT  
1552    using slot=6, which is an illegal slot, as only 1, 3, 5 are permitted.  
1553

1554

1555

1556

1557

1558

1559

1560

1561

1562

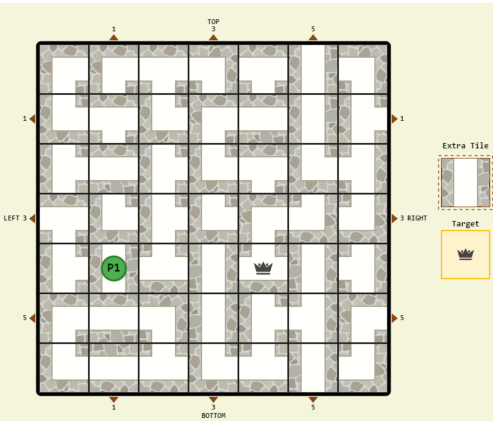
1563

1564

1565

1566  
1567

## Shallow Planning .

1568  
1569  
1570  
1571  
1572  
1573  
1574  
1575  
1576  
1577  
1578  
1579  
1580  
1581

The goal is to move P1 from (1,4) to the Crown at (4,4). The Extra Tile is I1 (horizontal corridor).

Current state:

- P1 is at (1,4). The tile at (1,4) is a T-shape (N, E, S).
- Crown is at (4,4). The tile at (4,4) is an L-shape (S, W).
- The path in row 4 is blocked:
  - (1,4) opens East.
  - (2,4) is an L-shape (E, S). It does NOT open West, so P1 cannot move to (2,4).
  - (3,4) is an L-shape (N, E). It does NOT open West.
  - (4,4) opens West.

The strategy is to use the Extra Tile (I1) to create a horizontal path in row 4. Since row 4 is not a shove-able row, we need to manipulate the board using shove-able columns (1, 3, 5) or rows (1, 3, 5).

1582

Let's try to insert the I1 tile into column 3 to replace one of the blocking tiles in row 4.

1583

\*\*Turn 1:\*\*  
1. \*\*INSERT:\*\* Insert the Extra Tile (I1, horizontal) into column 3 from the top. This will shift column 3 downwards.

- 'INSERT(side=top', slot=3, rotation=1)' (rotation 1 for I1 is horizontal)
- The I1 tile will be inserted at (3,0).
- The tile at (3,0) (L0) is ejected from the bottom. The new Extra Tile becomes L0.
- The tile at (3,3) (L1, E, S) moves to (3,4).
- The tile at (3,4) (L0, N, E) moves to (3,5).
- The tile at (3,5) (L2, S, W) moves to (3,6).
- The tile at (3,6) (L1) is ejected. (Correction: the tile at (3,6) is ejected, and the new extra tile is the one that was at (3,6), which is L1).
- P1 remains at (1,4). The Crown remains at (4,4).

After this insertion, the tile at (3,4) is now the original tile from (3,3), which is an L-shape (E, S).

1589

Let's check the path in row 4:

- (1,4) T-shape (N, E, S) - opens East.
- (2,4) L-shape (E, S) - does NOT open West. (Still blocked here)
- (3,4) L-shape (E, S) - opens East.
- (4,4) L-shape (S, W) - opens West.

The path is still blocked between (1,4) and (2,4).

1594

Let's try a different approach. We need to get a horizontal tile into (2,4) or (3,4).

1595

The Extra Tile is currently I1.

\*\*Turn 1 (Revised Strategy):\*\*

Let's try to insert the I1 tile into column 1 from the bottom. This will shift P1's tile.

1596

1. \*\*INSERT:\*\* Insert the Extra Tile (I1, horizontal) into column 1 from the bottom.

- 'INSERT(side=bottom', slot=1, rotation=1)'
- The I1 tile will be inserted at (1,6).
- The tile at (1,6) (L2) is ejected from the top. The new Extra Tile becomes L2.
- P1's tile at (1,4) (T-shape, N, E, S) moves to (1,5). So P1 is now at (1,5).
- The tile at (1,3) (L3, W, N) moves to (1,4).
- The tile at (1,2) (L0, N, E) moves to (1,3).
- The tile at (1,1) (L1, E, S) moves to (1,2).
- The tile at (1,0) (L3, W, N) moves to (1,1).
- The new tile at (1,0) is the I1 tile. (Correction: The I1 tile is inserted at (1,6), not (1,0). The tile at (1,0) is shifted to (1,1).

The tile at (1,6) is ejected. The new I1 tile is inserted at (1,6).

1604

Let's re-evaluate the initial board and the goal.

1605

1606

1607

1608

1609

Figure 25: A reasoning trace from  Gemini 2.5 Flash on the  M-MAZE task, demonstrating a **shallow planning error**. The model fails to narrow the search space, producing an overly verbose reasoning trace that explores multiple incorrect `INSERT` actions. This exhaustive but aimless exploration continues until the token budget is reached, ultimately resulting in a failure to output any valid plan.

1610

1611

1612

1613

1614

1615

1616

1617

1618

1619

1620  
 1621  
 1622  
 1623  
 1624  
 1625  
 1626  
 1627  
 1628  
 1629  
 1630  
 1631  
 1632  
 1633  
 1634  
 1635  
 1636  
 1637  
 1638  
 1639  
 1640  
 1641  
 1642  
 1643  
 1644  
 1645  
 1646  
 1647  
 1648  
 1649  
 1650  
 1651  
 1652  
 1653  
 1654  
 1655  
 1656  
 1657  
 1658  
 1659  
 1660  
 1661  
 1662  
 1663  
 1664  
 1665  
 1666  
 1667  
 1668  
 1669  
 1670  
 1671  
 1672  
 1673

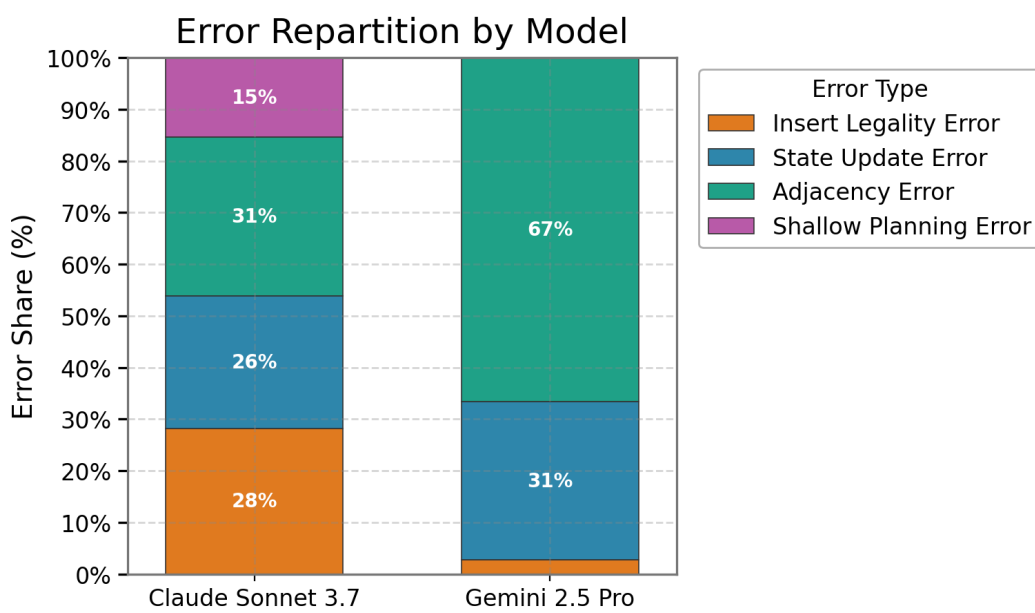


Figure 26: Error composition for Claude Sonnet 3.7 & Gemini 2.5 Pro on the MAZE Easy (Oracle Parsing) task. The stacked bar shows each category's share of all annotated failures (N=25).